

Recent Progresses in Quarkonium Production



**Hee Sok Chung
Korea University**

QNP2022 - The 9th International Conference on Quarks and Nuclear Physics
5-9 September 2022
online

Nonrelativistic QCD

- NRQCD provides a description of a heavy quarkonium state $|Q\rangle$ as nonrelativistic Fock state expansion

$$|Q\rangle = O(1)|Q\bar{Q}\rangle + O(v)|Q\bar{Q}g\rangle + O(v^2)|Q\bar{Q}gg\rangle + \dots$$

$v^2 \approx 0.3$ for charmonia,

$v^2 \approx 0.1$ for bottomonia.

Caswell, Lepage, PLB167, 437 (1986)

**Bodwin, Braaten, Lepage, PRD51, 1125 (1995),
PRD55, 5853 (1997)**

- LO in v : the leading Fock state is $Q\bar{Q}$ in a color-singlet state.
- Contributions at higher orders can involve **color-octet states**.
- NRQCD have been successfully applied to spectroscopy and decay processes.

NRQCD Factorization

- Inclusive production cross section of a quarkonium \mathcal{Q}

Short-distance cross sections  **Long-distance matrix elements** 

$$\sigma_{\mathcal{Q}+X} = \sum_n \hat{\sigma}_{Q\bar{Q}(n)+X} \langle \mathcal{O}^{\mathcal{Q}}(n) \rangle$$

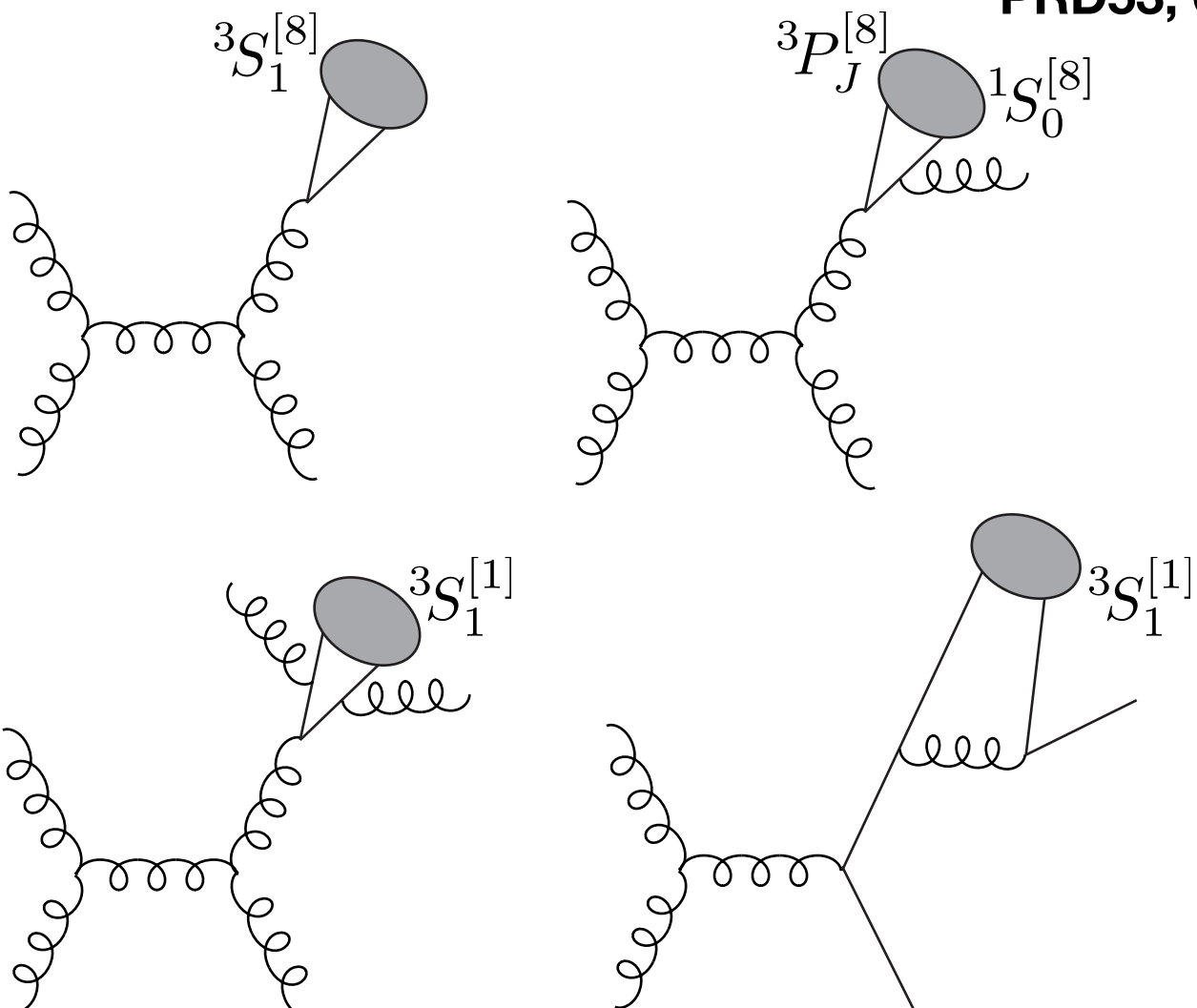
- Sum is over the color, spin, and orbital angular momentum states of the $Q\bar{Q}$.
- Matrix elements have known scalings in v .
- For a S -wave spin-triplet quarkonium,
Leading order in v : ${}^3S_1^{[1]}$ (color singlet)
Relative orders v^3, v^4 : ${}^1S_0^{[8]}, {}^3S_1^{[8]}, {}^3P_J^{[8]} \quad (J=0,1,2)$ (color octet)
- Factorization is expected to be valid at large p_T .

NRQCD Factorization

- At large p_T , contribution at leading order in v (color singlet channel) severely underestimates data.
The gap is filled by color-octet production, which is enhanced by short-distance cross sections.

Braaten and Fleming, PRL74, 3327 (1995)
Cho and Leibovich, PRD 53, 150 (1996)
PRD53, 6203 (1996)

- Color-octet production:



- Color-singlet production:

Production of J/ψ , $\psi(2S)$, Υ

- Production cross section of a 3S_1 quarkonium $V=J/\psi, \psi(2S), \Upsilon$

$$\begin{aligned}\sigma_{V+X} = & \hat{\sigma}_{Q\bar{Q}({}^3S_1^{[1]})} \langle \mathcal{O}^V({}^3S_1^{[1]}) \rangle + \hat{\sigma}_{Q\bar{Q}({}^3S_1^{[8]})} \langle \mathcal{O}^V({}^3S_1^{[8]}) \rangle \\ & + \hat{\sigma}_{Q\bar{Q}({}^1S_0^{[8]})} \langle \mathcal{O}^V({}^1S_0^{[8]}) \rangle + \sum_{J=0,1,2} \hat{\sigma}_{Q\bar{Q}({}^3P_J^{[8]})} (2J+1) \langle \mathcal{O}^V({}^3P_0^{[8]}) \rangle.\end{aligned}$$

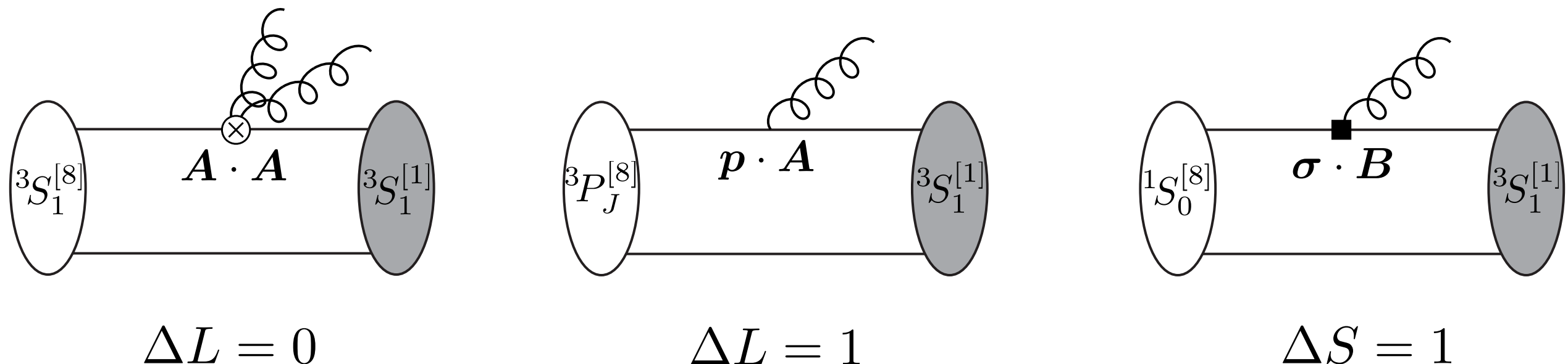
- The color-singlet matrix element $\langle \mathcal{O}^V({}^3S_1^{[1]}) \rangle$ can be obtained from decay rates, lattice QCD, or potential models.

$$\langle \mathcal{O}^V({}^3S_1^{[1]}) \rangle = \frac{3N_c}{2\pi} |R(0)|^2$$

- It is not known how to compute color-octet matrix elements from first principles, so they are usually extracted from cross section data : three unknowns for each 3S_1 quarkonium state.
- “NRQCD predictions” depend strongly on matrix element determinations

Color-octet matrix elements

- Color-octet matrix elements roughly correspond to probabilities for color-octet $Q\bar{Q}$ to evolve into a quarkonium.



- The ${}^3S_1^{[8]}$ and ${}^3P_J^{[8]}$ channels mix under scale variation :

$$\frac{d}{d \log \Lambda} \langle \mathcal{O}^V({}^3S_1^{[8]}) \rangle = \frac{6(N_c^2 - 4)}{N_c m^2} \frac{\alpha_s}{\pi} \langle \mathcal{O}^V({}^3P_0^{[8]}) \rangle$$

so that the sum of ${}^3S_1^{[8]}$ and ${}^3P_J^{[8]}$ channels is physically meaningful. Usually $\Lambda=m$ is taken in the $\overline{\text{MS}}$ scheme.

Production of J/ψ , $\psi(2S)$, Υ

- Matrix element determinations from cross section data rely heavily on the p_T shapes. This can be understood from expansion in $1/p_T$ ($p_T \gg m$)

$$\frac{d\sigma_H}{dp_T^2} = \sum_{i=g,q,\bar{q}} \frac{d\sigma_i}{dp_T^2} \otimes D_{i \rightarrow H}(z, \mu) \quad (\sim 1/p_T^4)$$

Leading-power fragmentation

$$+ \sum_n \frac{d\sigma_{Q\bar{Q}(n)}}{dp_T^2} \otimes D_{Q\bar{Q}(n) \rightarrow H}(z, \zeta_1, \zeta_2, \mu) \quad (\sim 1/p_T^6)$$

Next-to-leading-power fragmentation

$+O(1/p_T^8)$ J.C.Collins and D.E.Soper, NPB194, 445 (1982)
 Z.-B. Kang, J.-W. Qiu, G. Sterman, PRD 108, 102002 (2018)

Z.-B. Kang, J.-W. Qiu, G. Sterman, PRL108, 102002 (2012)

S. Fleming, A. K. Leibovich, T. Mehen, I. Z. Rothstein, PRD86, 094012 (2012)

Y.-Q. Ma, J.-W. Qiu, G. Sterman, H. Zhang, PRL113, 142002 (2014)

- Relative size of LP and NLP determines overall shape in p_T .
 - Two degrees of freedom in p_T shape constrains ***only two linear combinations*** of color-octet matrix elements. Need more constraints to determine all three matrix elements.

Potential NRQCD

Pineda, Soto, NPB Proc. Suppl. 64, 428 (1998)

Brambilla, Pineda, Soto, Vairo, NPB566, 275 (2000)

Brambilla, Pineda, Soto, Vairo, Rev. Mod. Phys. 77, 1423 (2005)

- Potential NRQCD effective field theory calculation of the color-octet matrix elements for strongly coupled quarkonia give

$$\langle \mathcal{O}^V(^3S_1^{[8]}) \rangle^{(\Lambda)} = \frac{1}{2N_c m^2} \frac{3|R(0)|^2}{4\pi} \mathcal{E}_{10;10}(\Lambda)$$

$$\langle \mathcal{O}^V(^3P_0^{[8]}) \rangle = \frac{1}{18N_c} \frac{3|R(0)|^2}{4\pi} \mathcal{E}_{00}$$

$$\langle \mathcal{O}^V(^1S_0^{[8]}) \rangle = \frac{1}{6N_c m^2} \frac{3|R(0)|^2}{4\pi} c_F^2(m; \Lambda) \mathcal{B}_{00}(\Lambda)$$

Universal gluonic correlators

short-distance coefficient
for spin-flip interaction

Brambilla, HSC, Vairo,
PRL126, 082003 (2021)
JHEP 09 (2021) 032

Brambilla, HSC,
Vairo, Wang,
PRD105, L111503
(2022)

- Gluonic correlators are vacuum expectation values of Wilson lines and field strengths; they are ***universal*** and ***independent*** of the heavy quark ***flavor*** or ***radial excitation***.
- This reduces the number of nonperturbative unknowns and *enhances the predictive power* : three nonperturbative unknowns determine ***all*** 3S_1 quarkonium cross sections

Potential NRQCD

- Universality of the gluonic correlators leads to the prediction for *cross section ratios*, independently of the correlators

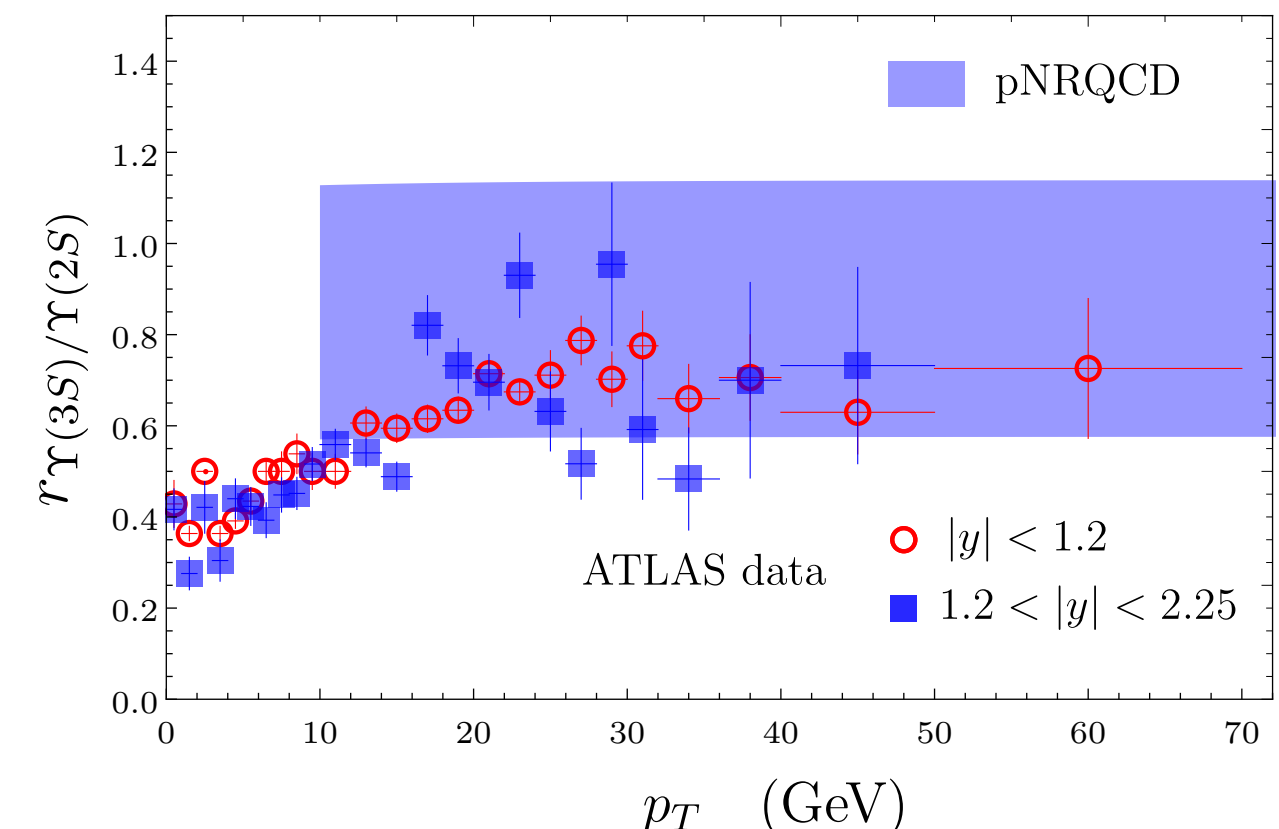
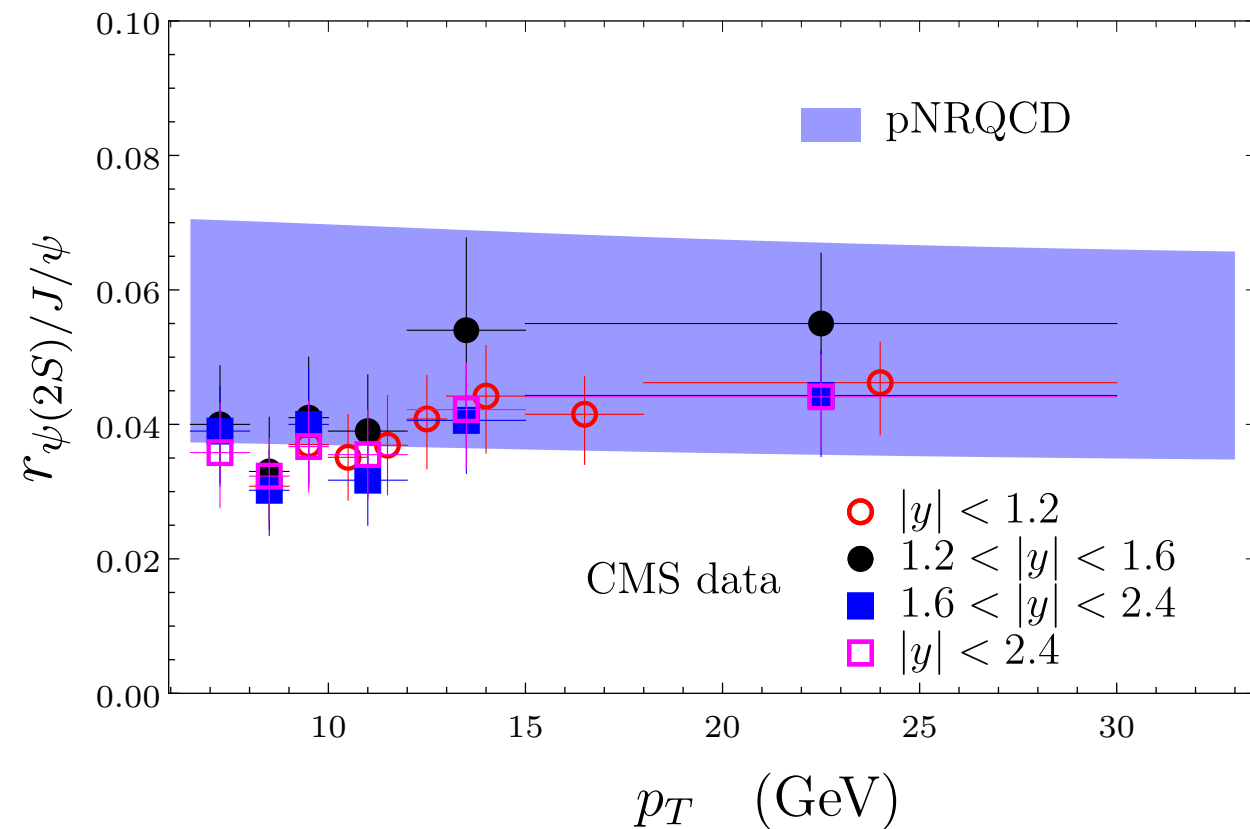
$$\frac{\sigma_{\psi(2S)}^{\text{direct}}}{\sigma_{J/\psi}^{\text{direct}}} = \frac{|R_{\psi(2S)}^{(0)}(0)|^2}{|R_{J/\psi}^{(0)}(0)|^2}$$

$$\frac{\sigma_{\Upsilon(3S)}^{\text{direct}}}{\sigma_{\Upsilon(2S)}^{\text{direct}}} = \frac{|R_{\Upsilon(3S)}^{(0)}(0)|^2}{|R_{\Upsilon(2S)}^{(0)}(0)|^2}$$

Brambilla, HSC,
Vairo, Wang,
PRD105, L111503
(2022)

- Compared to experiment, including feeddown effects:

$$r_{A/B} = (\text{Br}_{A \rightarrow \mu^+ \mu^-} \sigma_A) / (\text{Br}_{B \rightarrow \mu^+ \mu^-} \sigma_B)$$

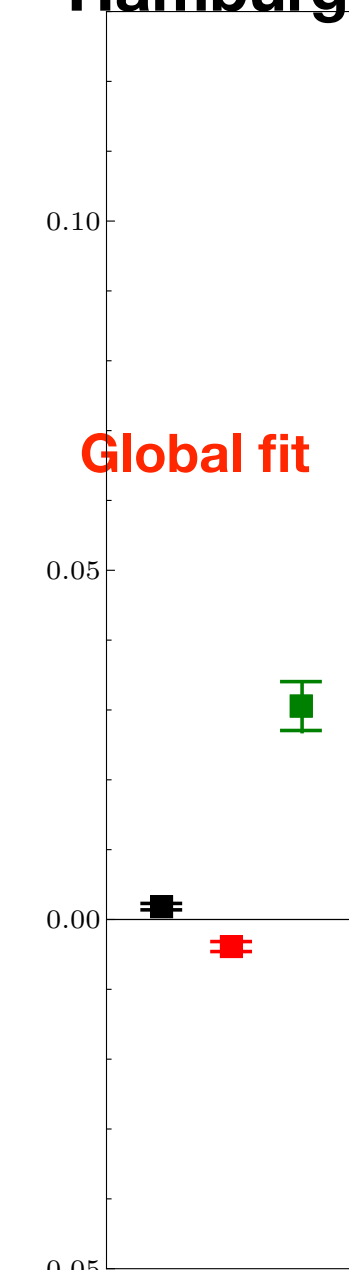


- Absolute cross sections require values of gluonic correlators

Matrix element determinations

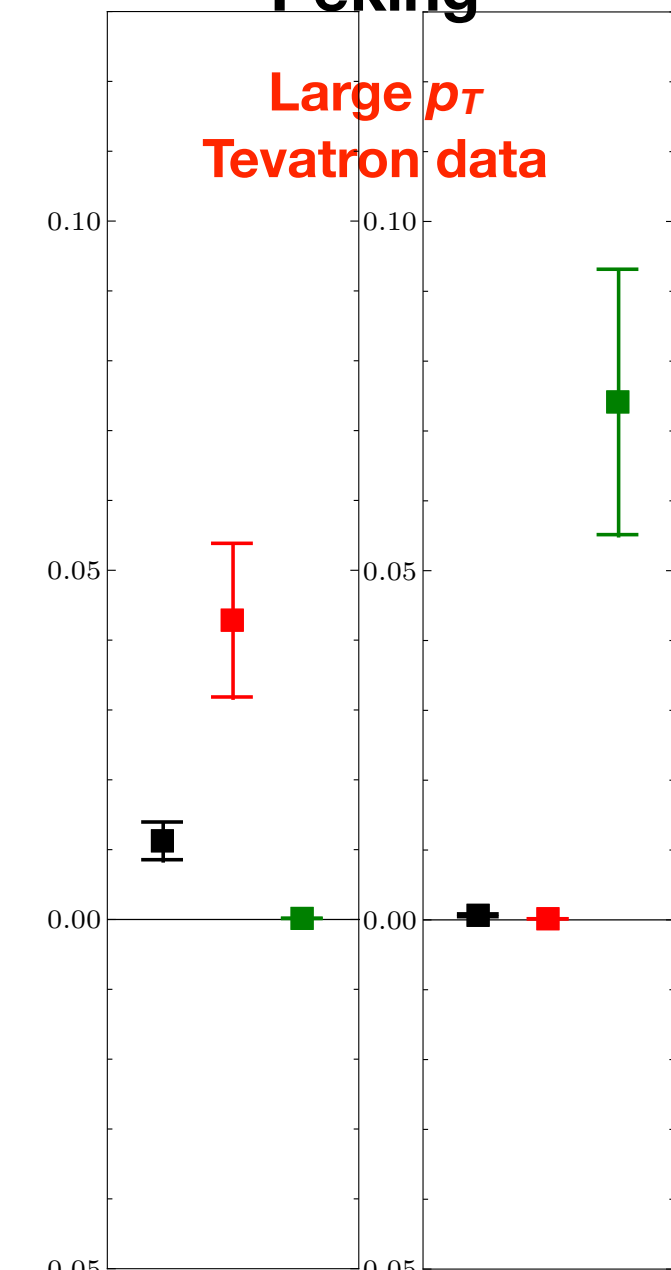
- J/ψ matrix elements $\langle \mathcal{O}^{J/\psi}(^3S_1^{[8]}) \rangle$, $\langle \mathcal{O}^{J/\psi}(^3P_0^{[8]}) \rangle/m^2$, $\langle \mathcal{O}^{J/\psi}(^1S_0^{[8]}) \rangle$ (GeV³)

Hamburg



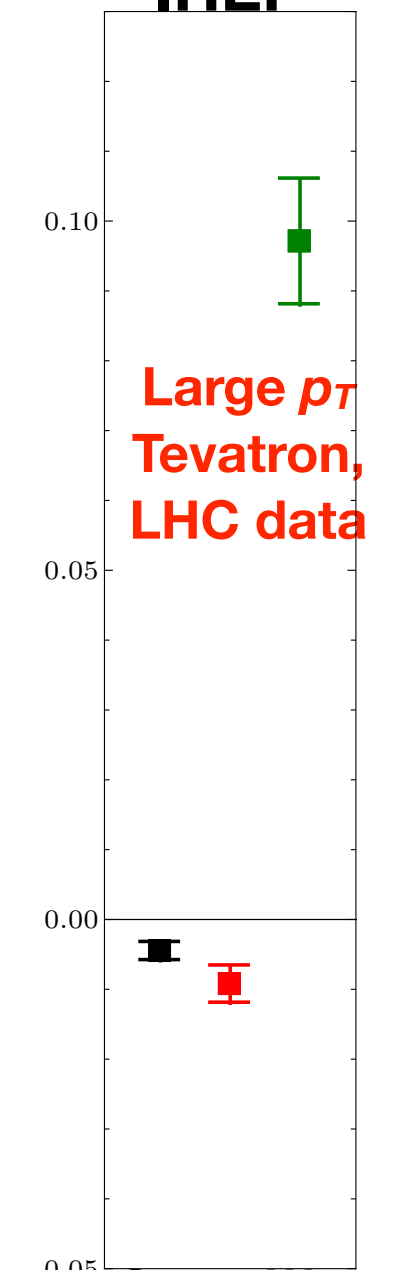
Butenschoen
and Kniehl,
PRD84, R051501
(2011)

Peking



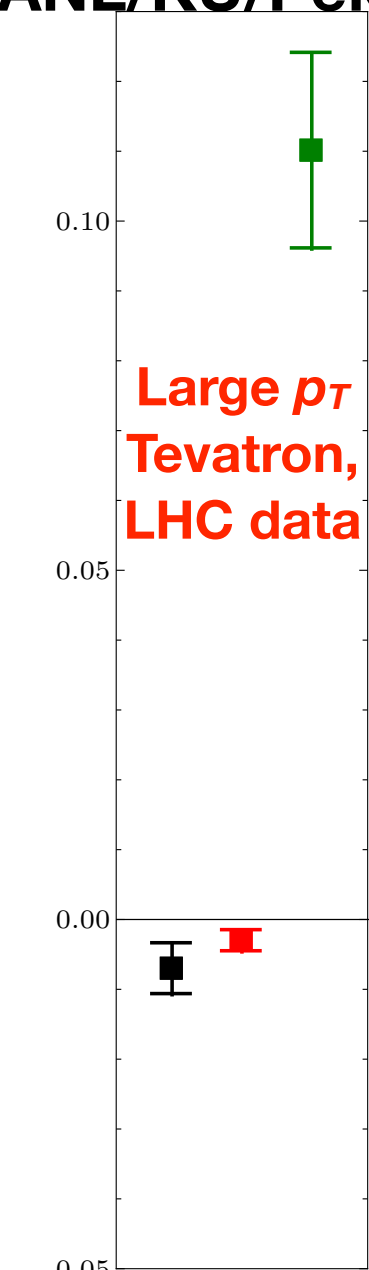
Shao, Han, Ma,
Meng, Zhang, Chao,
JHEP 1505 (2015) 103

IHEP



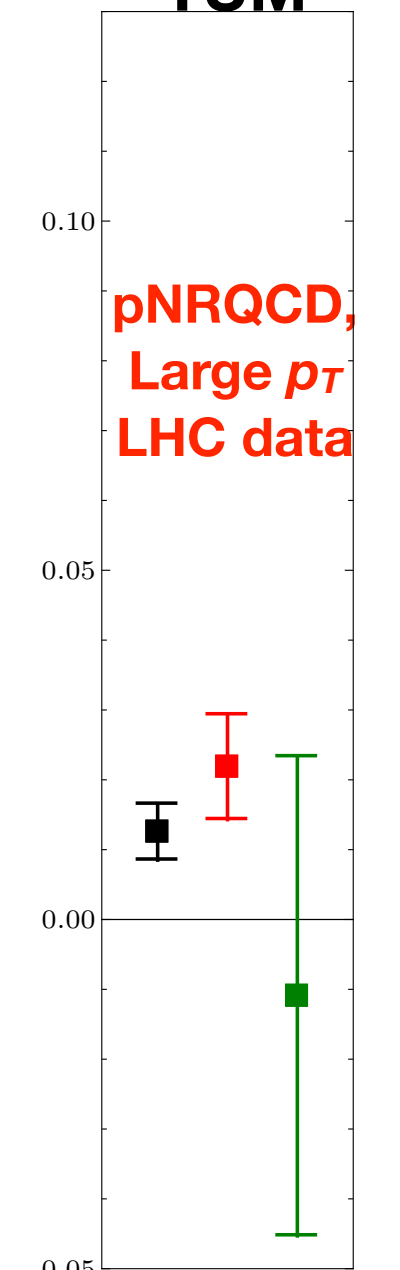
Gong, Wan,
Wang, Zhang,
Zhang (PRL110, 042002
10 (2013))

ANL/KU/Peking



Bodwin, Chao, HSC,
Kim, Lee, Ma,
PRD93, 034041
(2016)

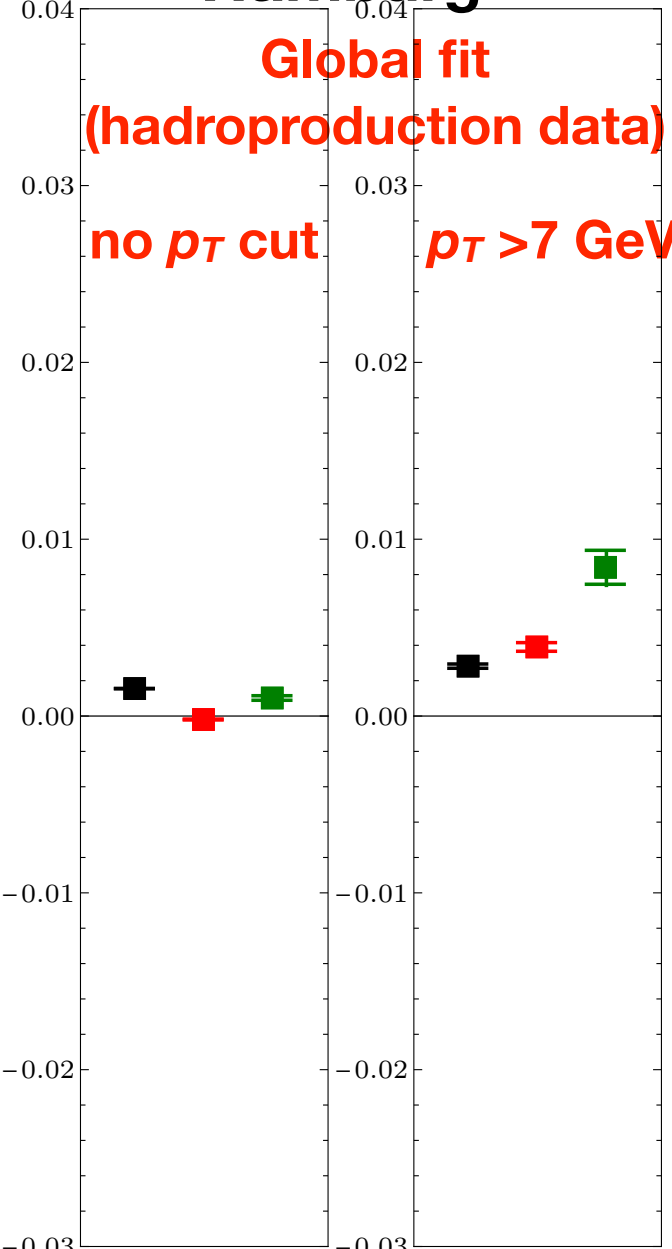
TUM



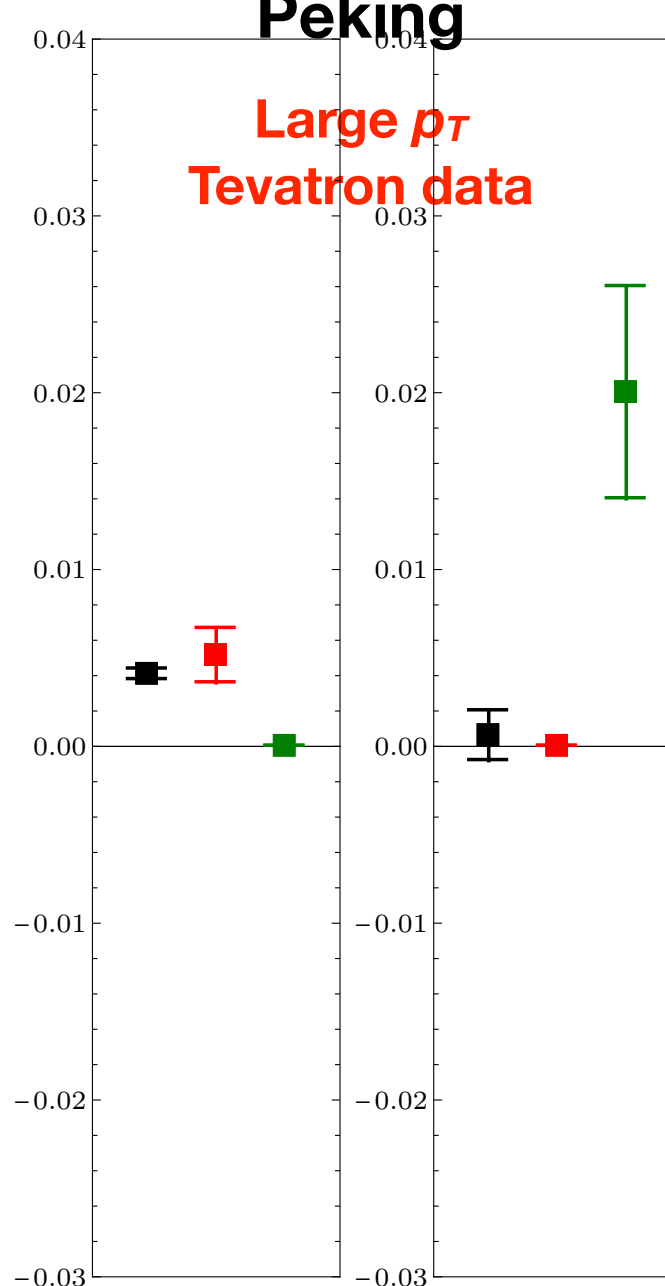
Brambilla, HSC,
Vairo, Wang,
PRD105, L111503
(2022)

Matrix element determinations

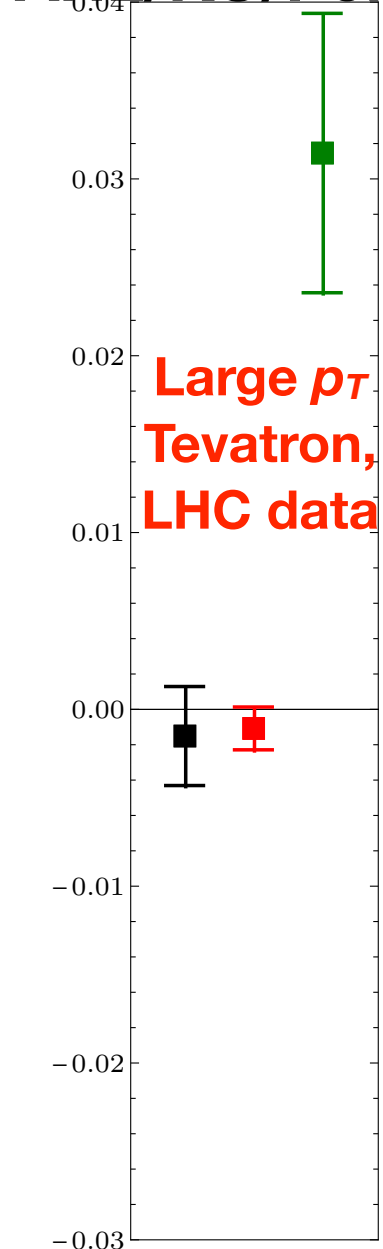
- $\psi(2S)$ matrix elements $\langle \mathcal{O}^{\psi(2S)}(^3S_1^{[8]}) \rangle$, $\langle \mathcal{O}^{\psi(2S)}(^3P_0^{[8]}) \rangle / m^2$, $\langle \mathcal{O}^{\psi(2S)}(^1S_0^{[8]}) \rangle$ (GeV³)

Hamburg

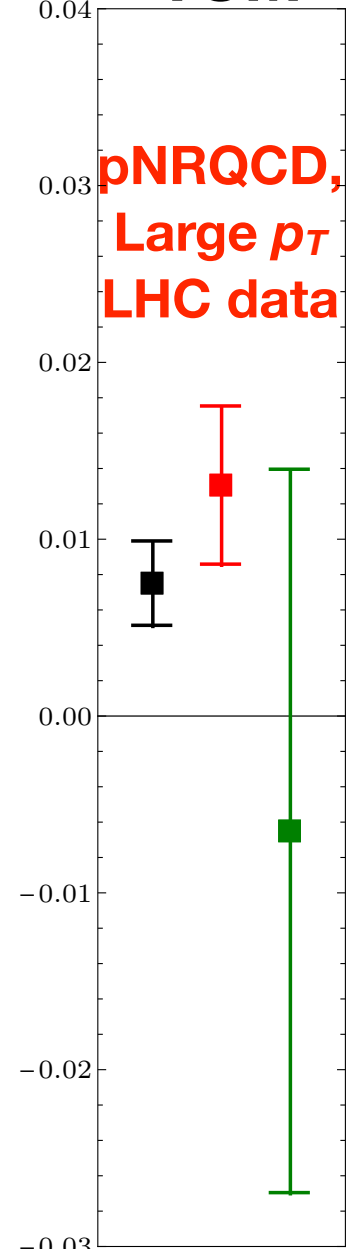
Butenschoen
and Kniehl,
2207.09346

Peking

Shao, Han, Ma,
Meng, Zhang, Chao,
JHEP 1505 (2015) 103
11

ANL/KU/Peking

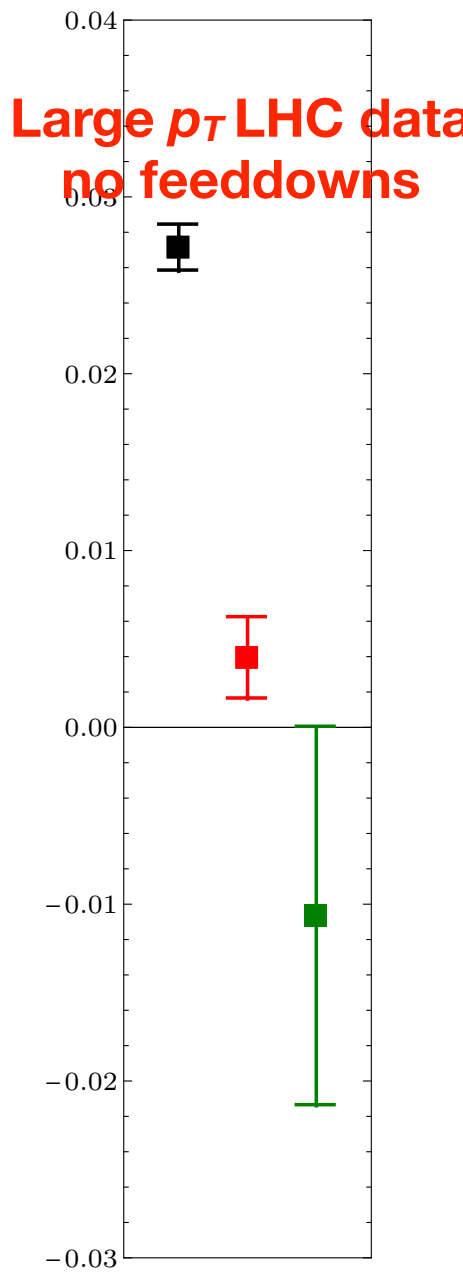
Bodwin, Chao, HSC,
Kim, Lee, Ma,
PRD93, 034041
(2016)

TUM

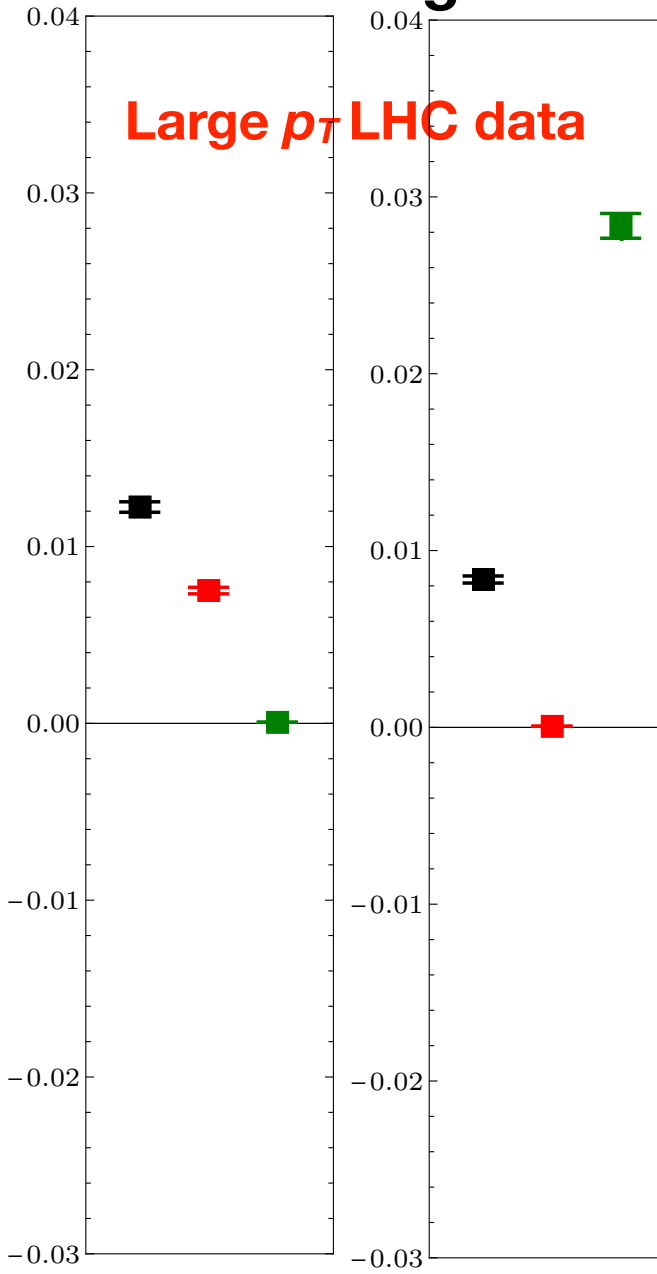
Brambilla, HSC,
Vairo, Wang,
PRD105, L111503
(2022)

Matrix element determinations

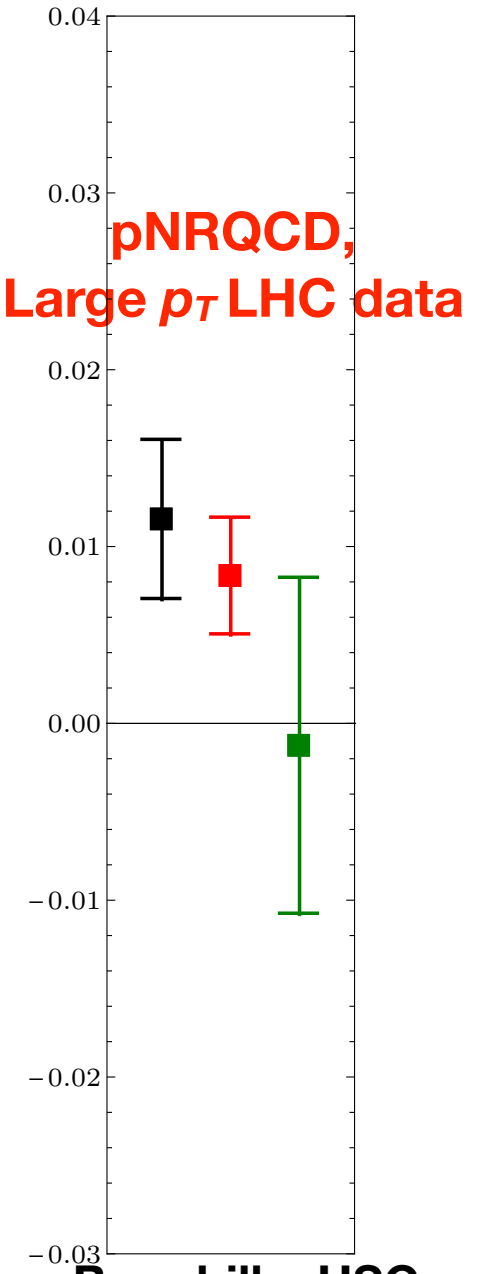
- $\Upsilon(3S)$ matrix elements $\langle \mathcal{O}^\Upsilon(^3S_1^{[8]}) \rangle$, $\langle \mathcal{O}^\Upsilon(^3P_0^{[8]}) \rangle/m^2$, $\langle \mathcal{O}^\Upsilon(^1S_0^{[8]}) \rangle$ (GeV³)

IHEP

Gong, Wan, Wang, Zhang,
PRL112, 032001 (2014)

Peking

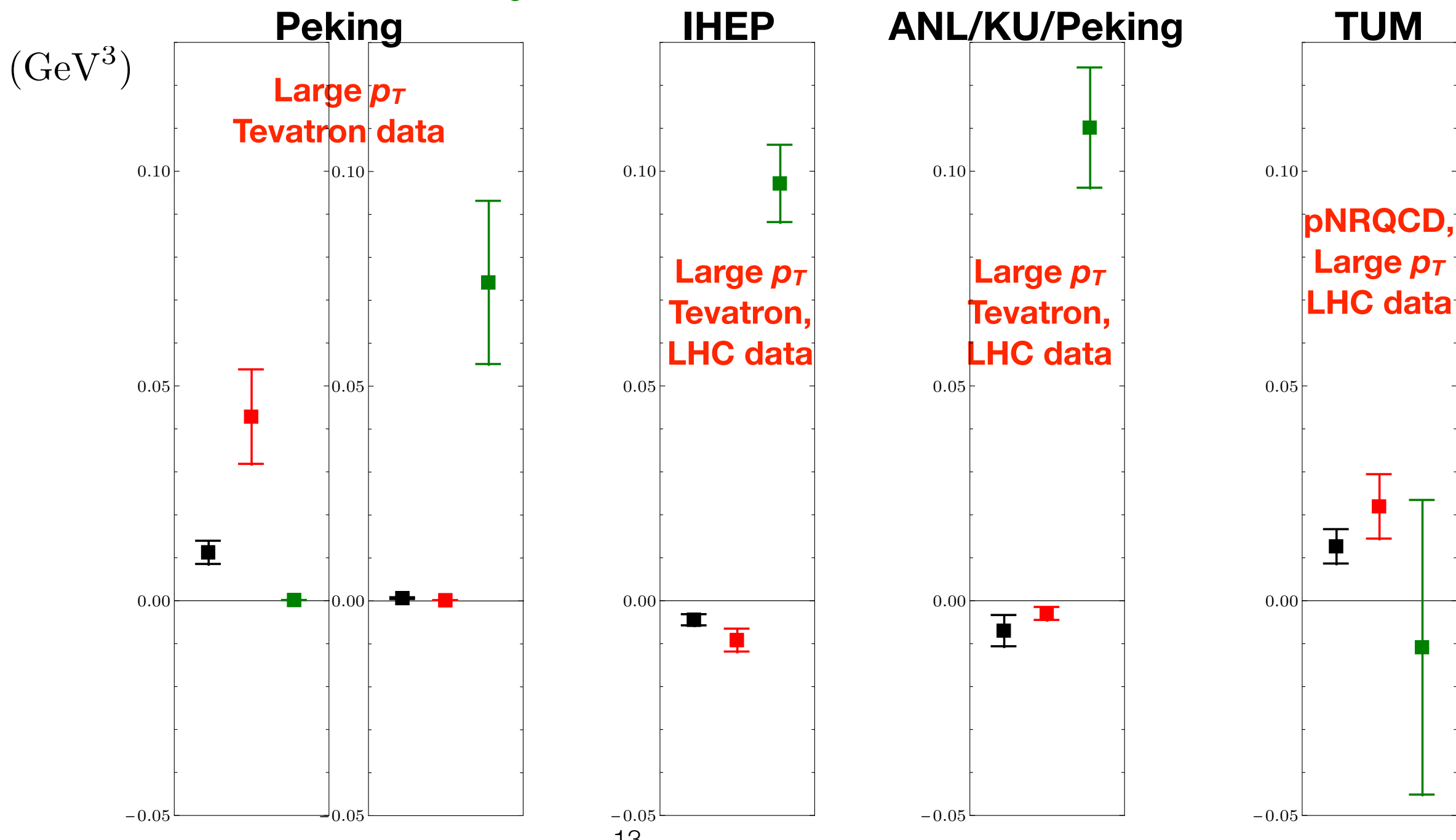
Han, Ma, Meng, Shao, Zhang, Chao,
PRD94, 014028 (2016)

TUM

Brambilla, HSC,
Vairo, Wang,
PRD105, L111503
(2022)

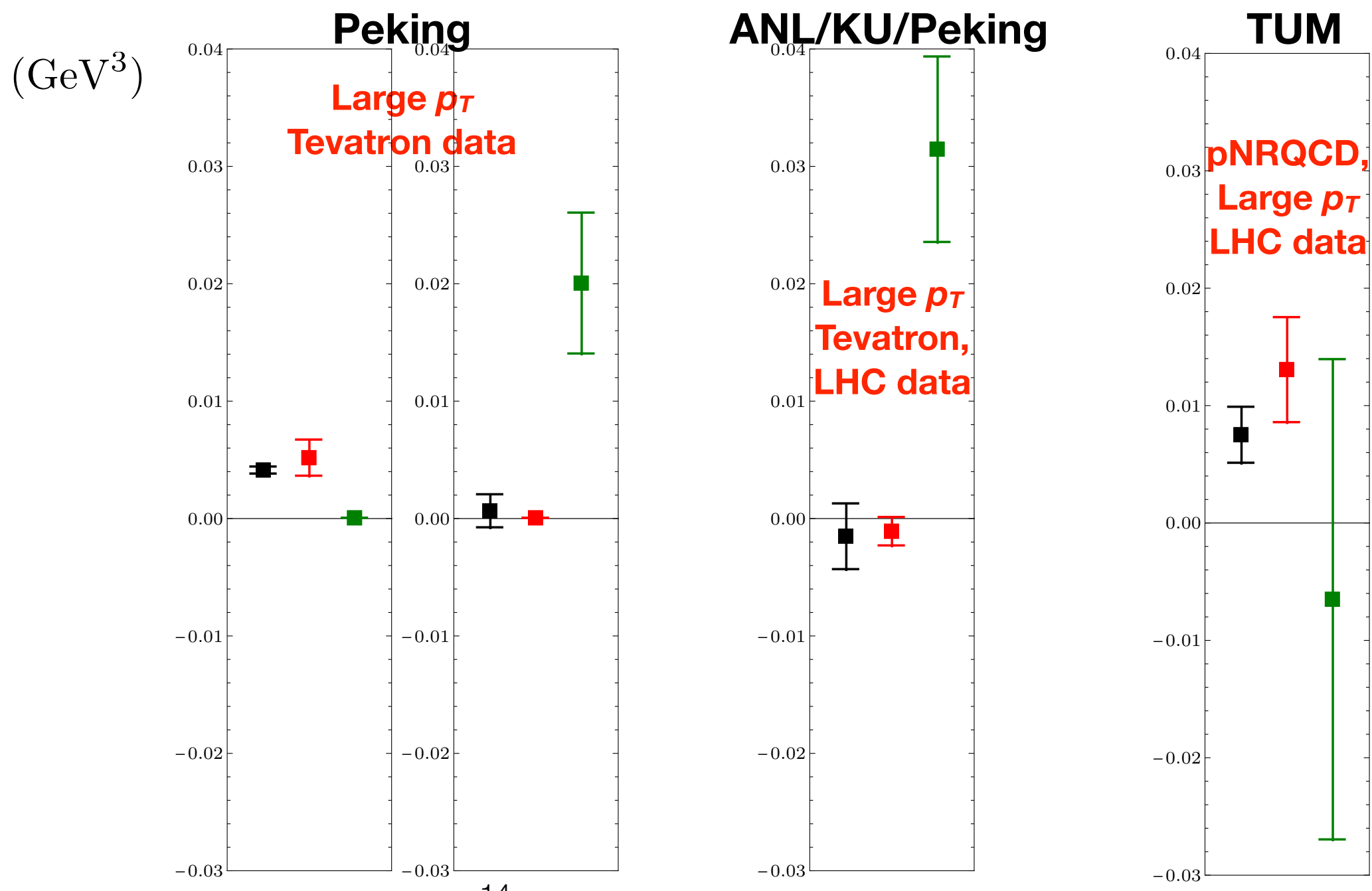
J/ψ Matrix elements from Large p_T Hadroproduction

- Same signs for $\langle \mathcal{O}^{J/\psi}(^3S_1^{[8]}) \rangle$ $\langle \mathcal{O}^{J/\psi}(^3P_0^{[8]}) \rangle/m^2$
- Poor control over $\langle \mathcal{O}^{J/\psi}(^1S_0^{[8]}) \rangle$



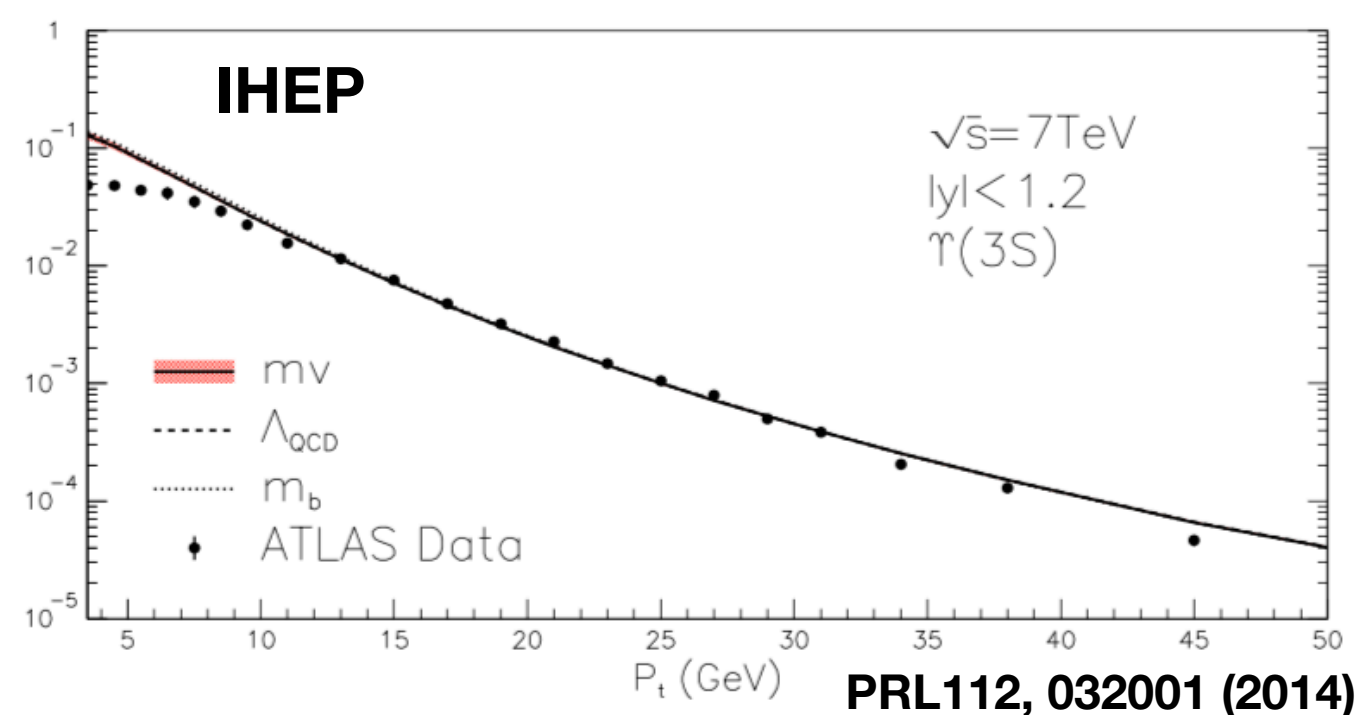
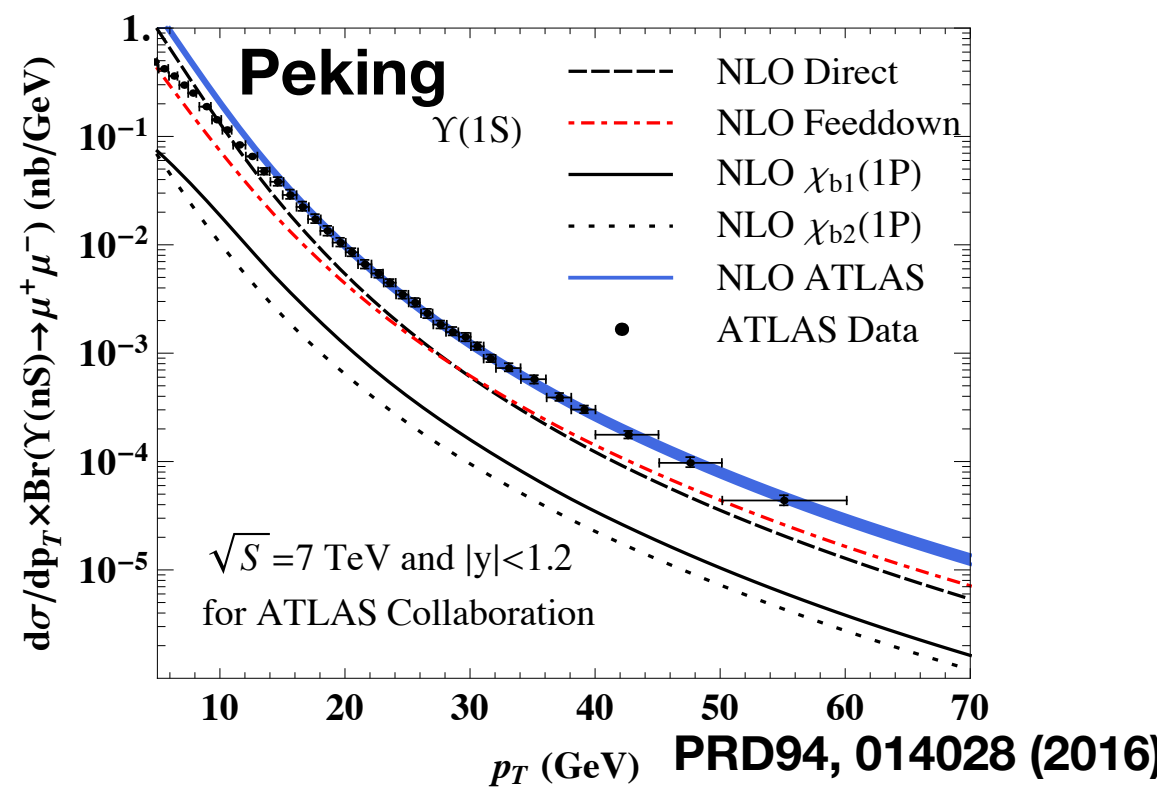
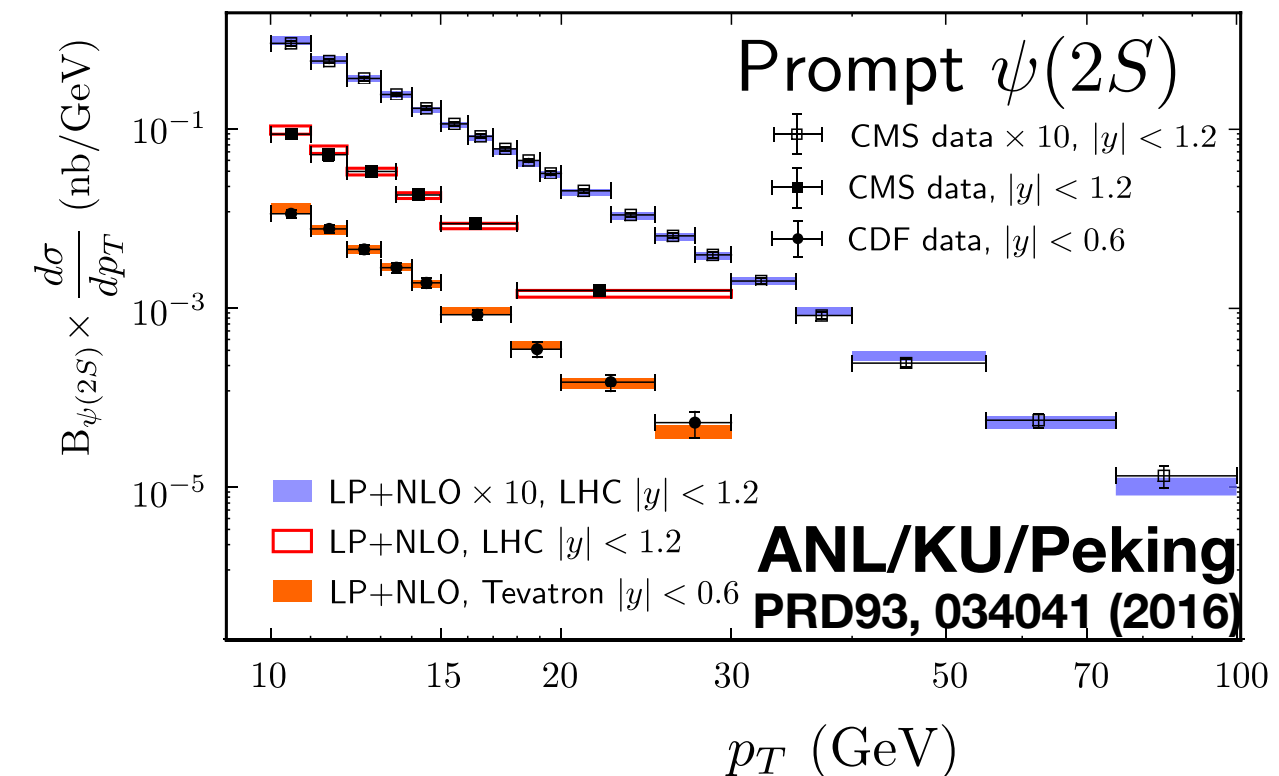
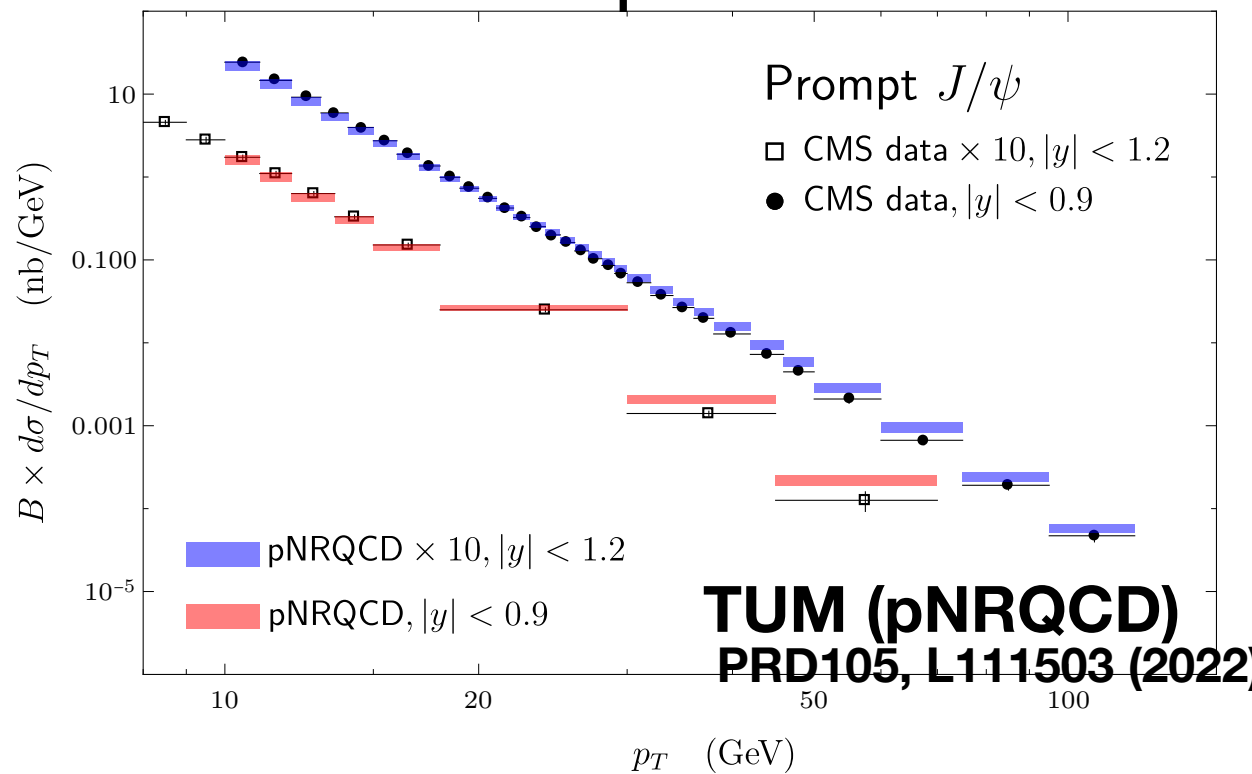
$\psi(2S)$ Matrix elements from Large p_T Hadroproduction

- Same signs for $\langle \mathcal{O}^{\psi(2S)}(^3S_1^{[8]}) \rangle$ $\langle \mathcal{O}^{\psi(2S)}(^3P_0^{[8]}) \rangle / m^2$
- Poor control over $\langle \mathcal{O}^{\psi(2S)}(^1S_0^{[8]}) \rangle$



Matrix elements from Large p_T Hadroproduction

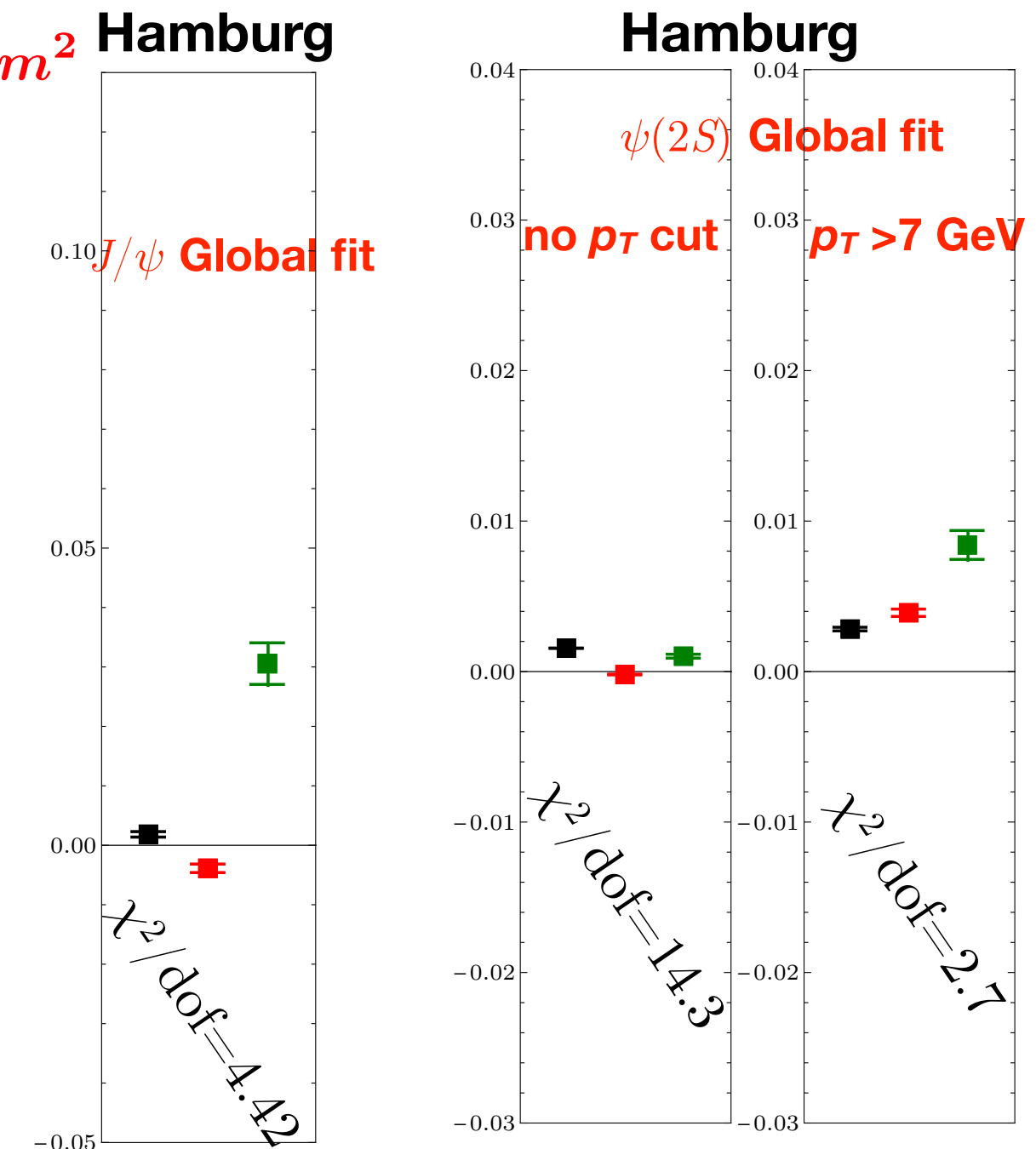
- Good description of cross section at large p_T .



Global Fit

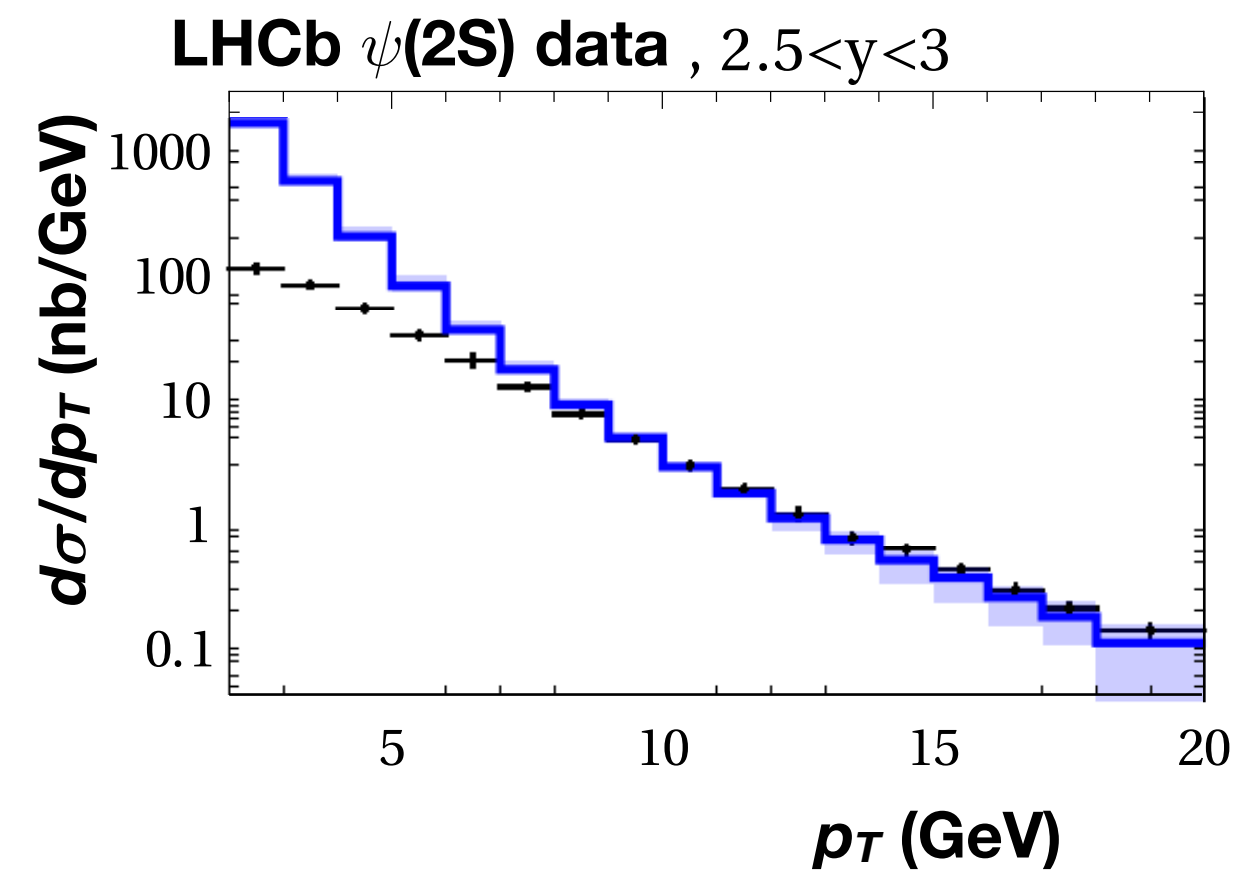
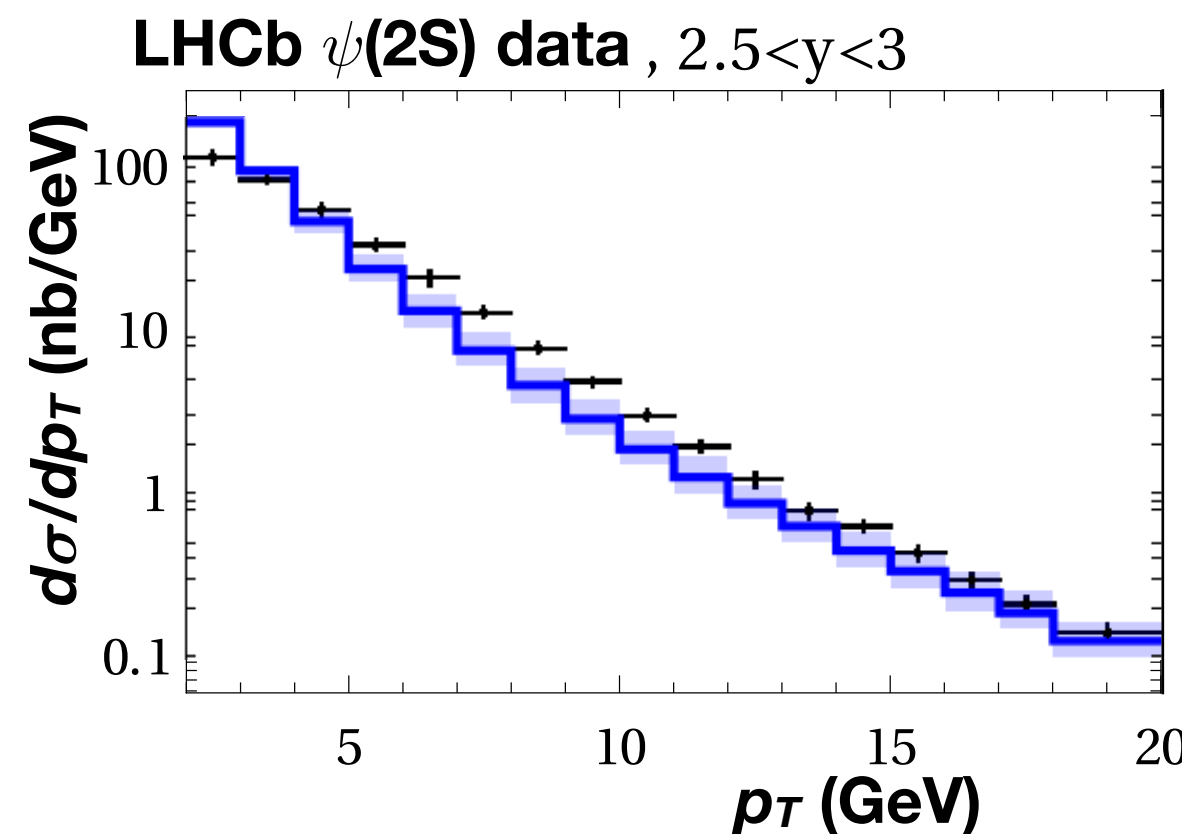
$$\langle \mathcal{O}^{J/\psi}(^3S_1^{[8]}) \rangle, \langle \mathcal{O}^{J/\psi}(^3P_0^{[8]}) \rangle/m^2, \langle \mathcal{O}^{J/\psi}(^1S_0^{[8]}) \rangle \text{ (GeV}^3\text{)}$$

- J/ψ global fit mainly from low- p_T data, gives negative $\langle \mathcal{O}^{J/\psi}(^3P_0^{[8]}) \rangle/m^2$
- $\psi(2S)$ global fit only comes from hadroproduction, results without p_T cut gives negative $\langle \mathcal{O}^{\psi(2S)}(^3P_0^{[8]}) \rangle/m^2$
- $\psi(2S)$ with $p_T > 7 \text{ GeV}$ similar to large p_T hadroproduction based results, $\langle \mathcal{O}^{\psi(2S)}(^3P_0^{[8]}) \rangle/m^2$ is now positive. Quality of fit also improves with p_T cut.



Global Fit

- Description of hadroproduction improves with p_T cut, but uncertainties increase at large p_T



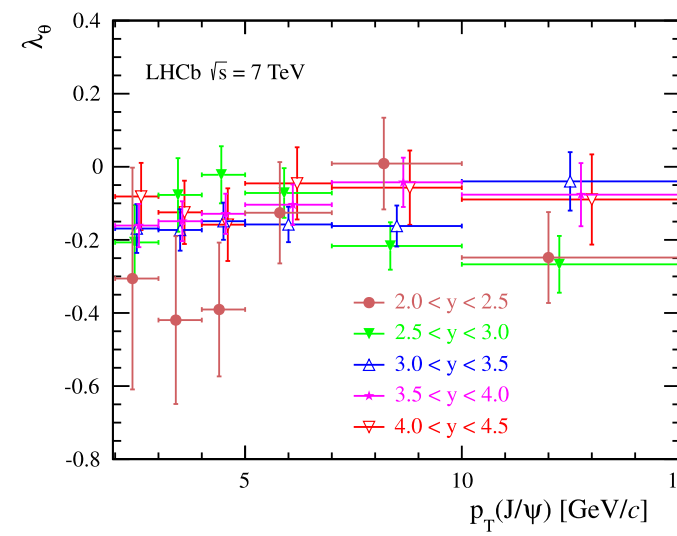
Hamburg
(Global fit, no p_T cut)
2207.09346

Hamburg
(Global fit, $p_T > 7$ GeV)
2207.09346

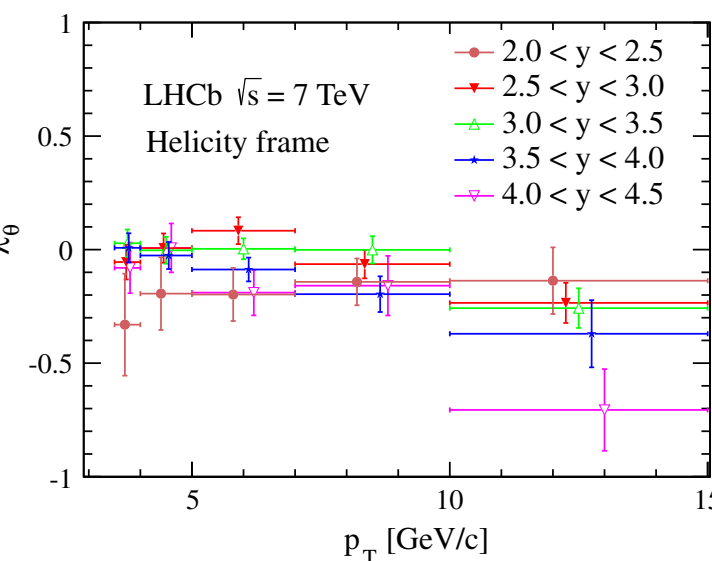
Quarkonium Polarization

- The polarization of the quarkonium can discriminate between different octet channels. This can be measured through the polar angular distribution of the dilepton decay $\sim 1 + \lambda_\theta \cos^2\theta$
- The polarization measured at the LHC show near-zero λ_θ (helicity frame)

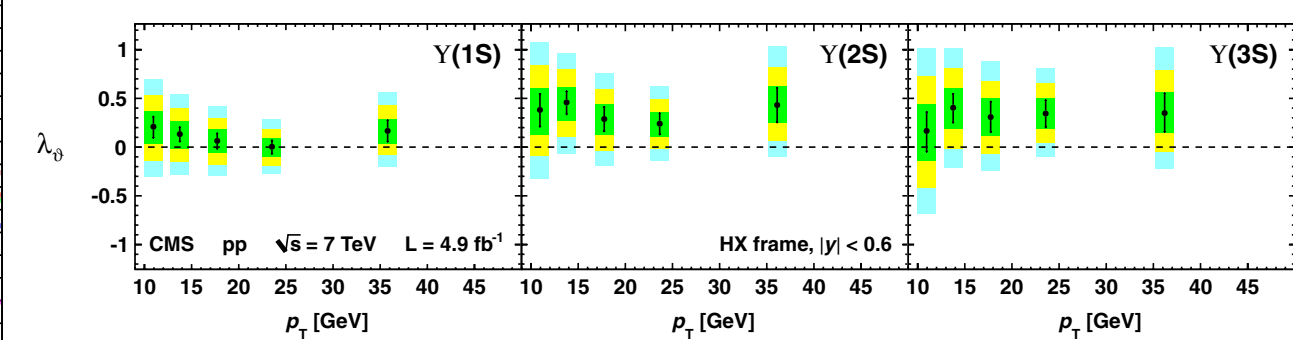
LHCb EPJC (2013) 73:2631



LHCb EPJC (2014) 74:2872

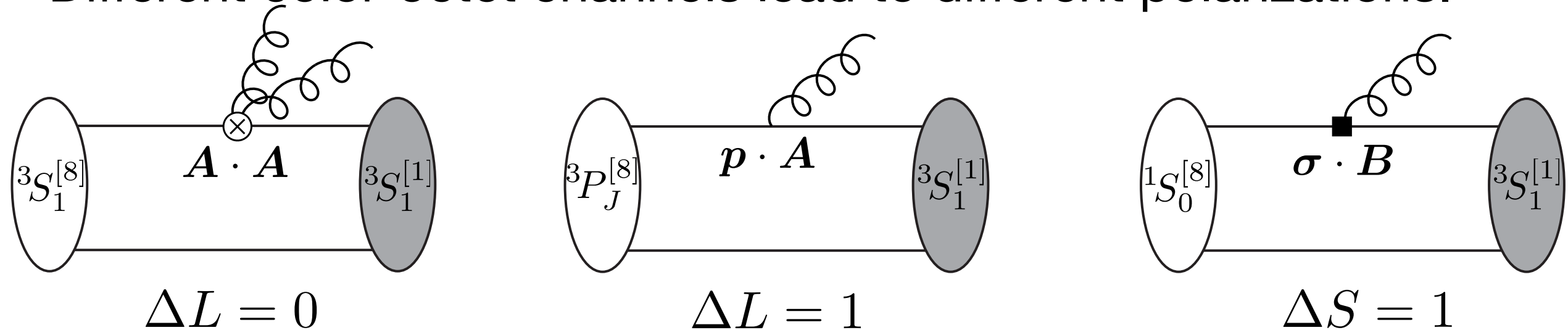


CMS PRL110, 081802



Quarkonium Polarization

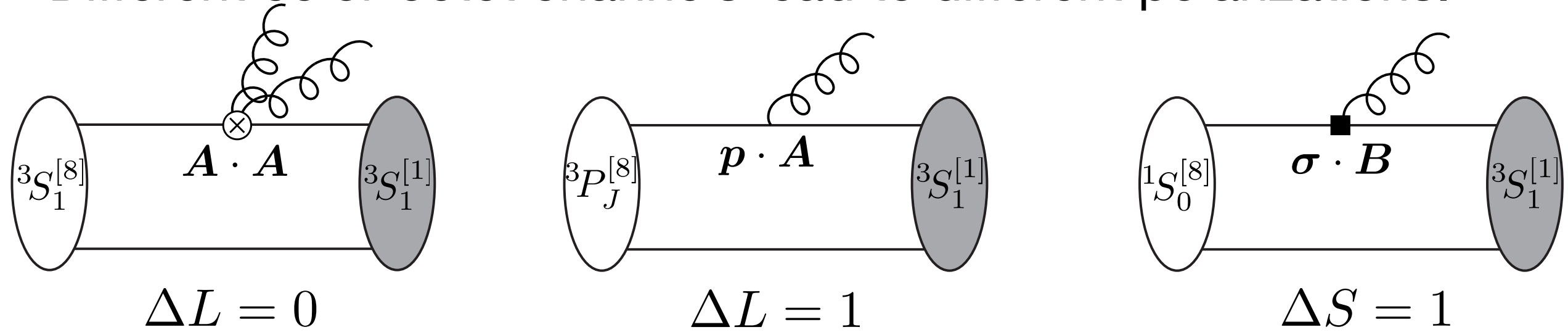
- Different color-octet channels lead to different polarizations.



- $Q\bar{Q}(^3S_1^{[8]})$ can produce a quarkonium by soft gluon emission : mostly transverse, small longitudinal contribution
- $Q\bar{Q}(^3P_1^{[8]})$ also evolves into a quarkonium by soft gluon emission, but short-distance coefficient is negative : mostly negatively transverse, small positive longitudinal contribution
- $Q\bar{Q}(^1S_0^{[8]})$ is isotropic, unpolarized.

Quarkonium Polarization

- Different color-octet channels lead to different polarizations.



**Large positive transverse,
small positive longitudinal**

**Large negative transverse,
small positive longitudinal**

unpolarized

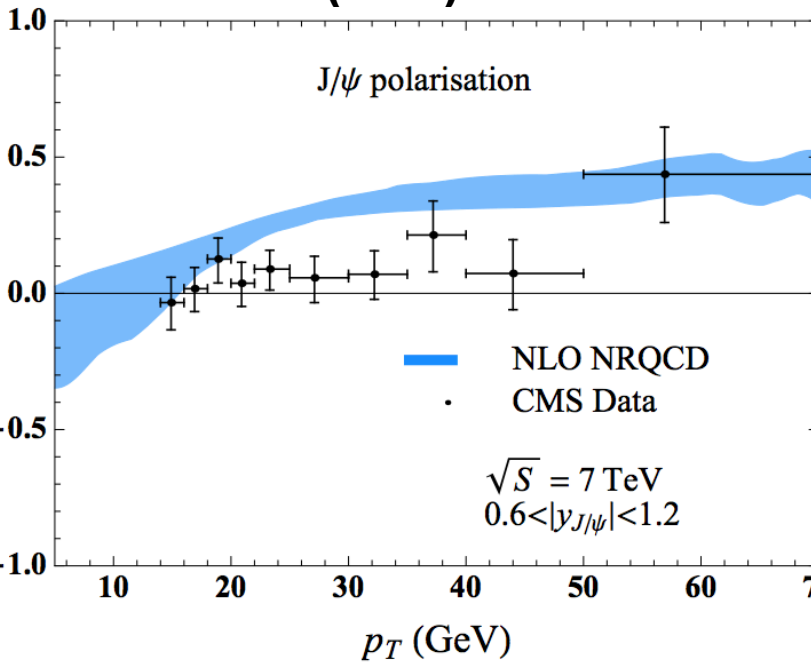
- To get near-zero λ_θ , we need either
 - $^1S_0^{[8]}$ dominates, while sum of $^3S_1^{[8]}$ and $^3P_J^{[8]}$ is small
 - $^3S_1^{[8]} + ^3P_J^{[8]}$ dominates despite large cancellations, small $^1S_0^{[8]}$
- For cancellations to happen in $^3S_1^{[8]} + ^3P_J^{[8]}$, the matrix elements must have same signs.

J/ψ Polarization

- Hadroproduction-based determinations generally lead to good descriptions of polarization. Global fit does not.

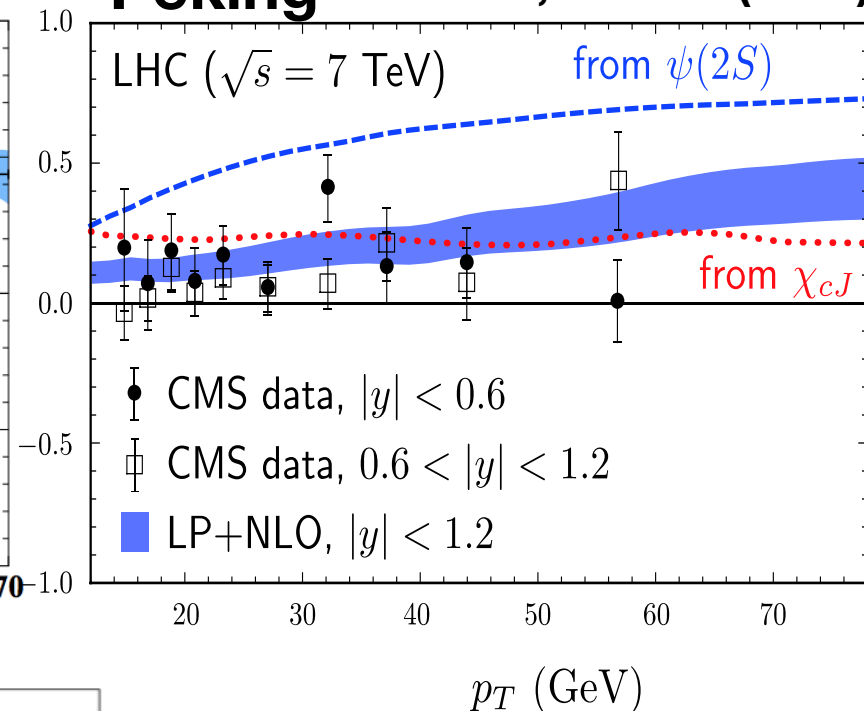
Peking

JHEP 1505 (2015) 103



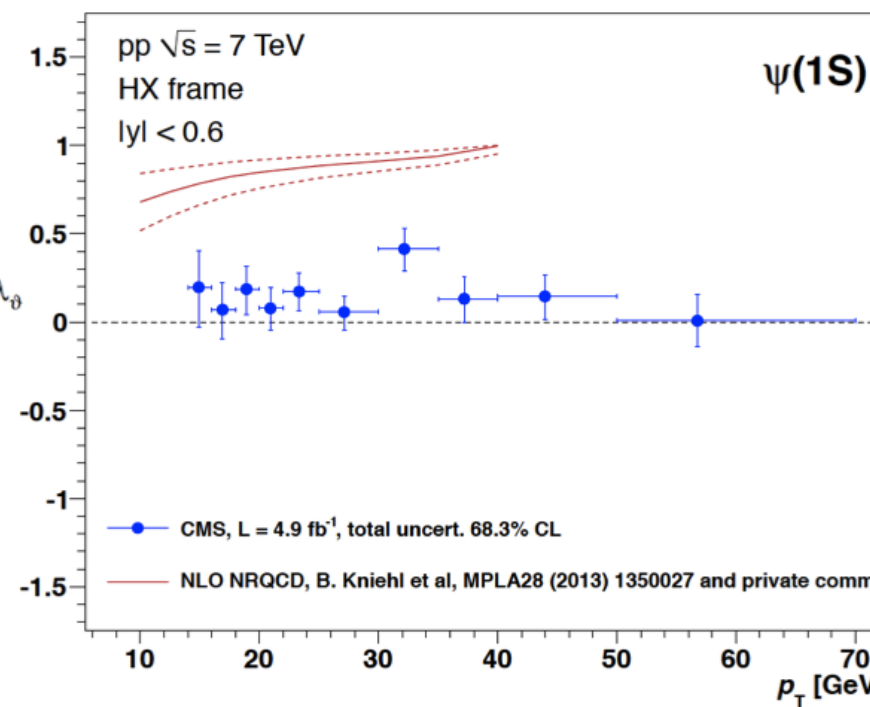
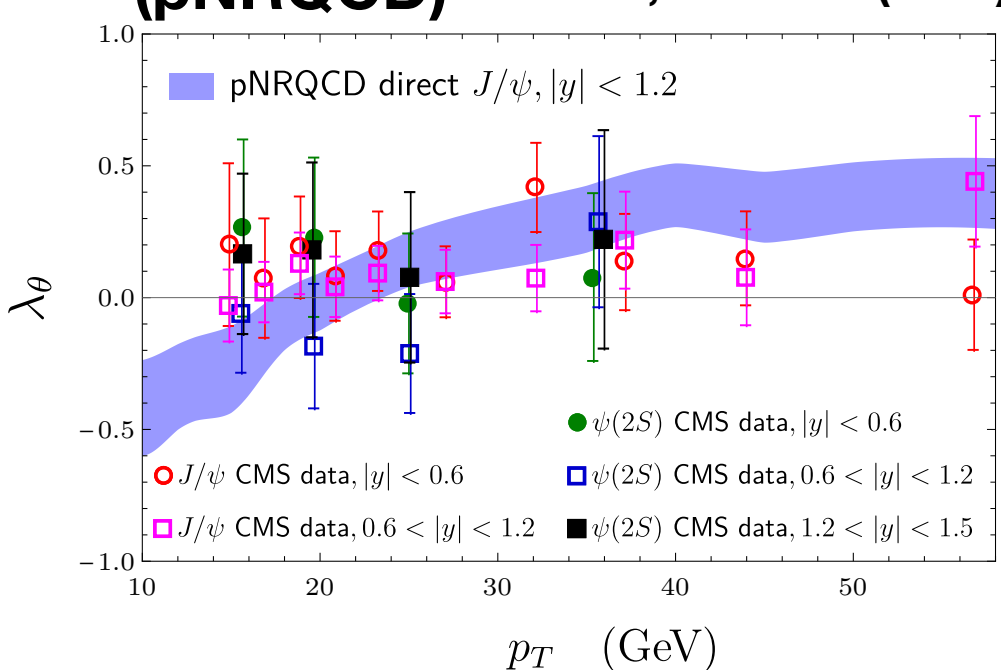
ANL/KU/

Peking PRD93, 034041 (2016)



TUM

(pNRQCD) PRD105, L111503 (2022)



**Hamburg
(Global fit)**

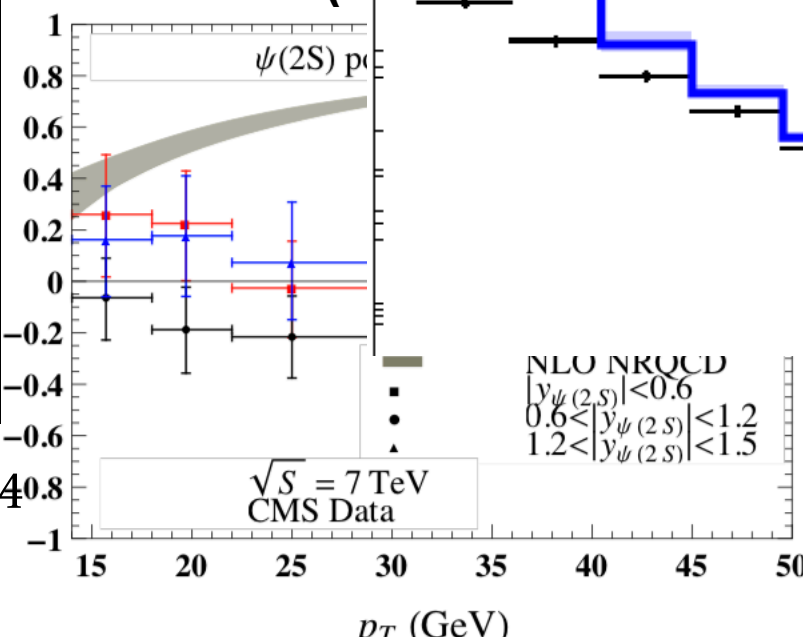
CMS, PLB727, 381 (2013)
Butenschoen and Kniehl, PRL108, 172002 (2012)

$\psi(2S)$ Polarization

- Hadroproduction-based determinations generally lead to good descriptions of polarization. Global fit without p_T cut does not.

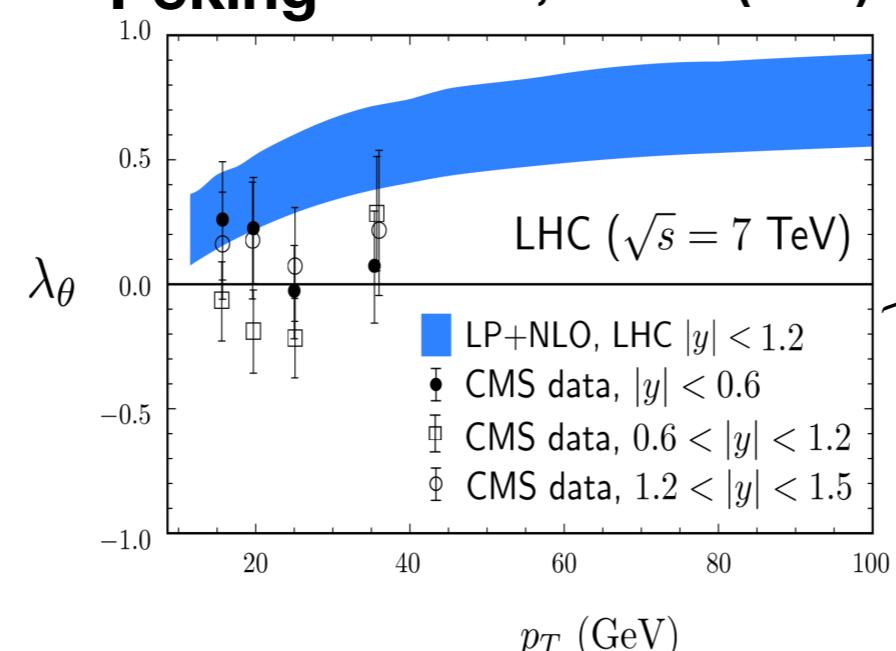
Peking

JHEP 1505 (2015) 103



ANL/KU/

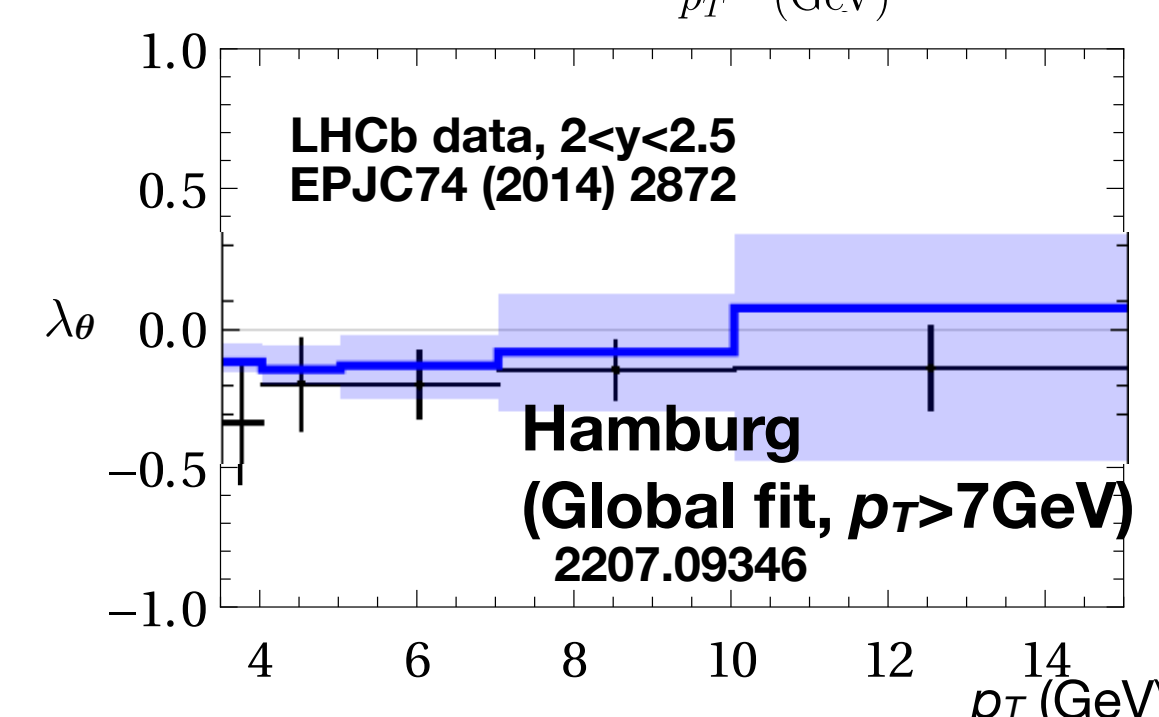
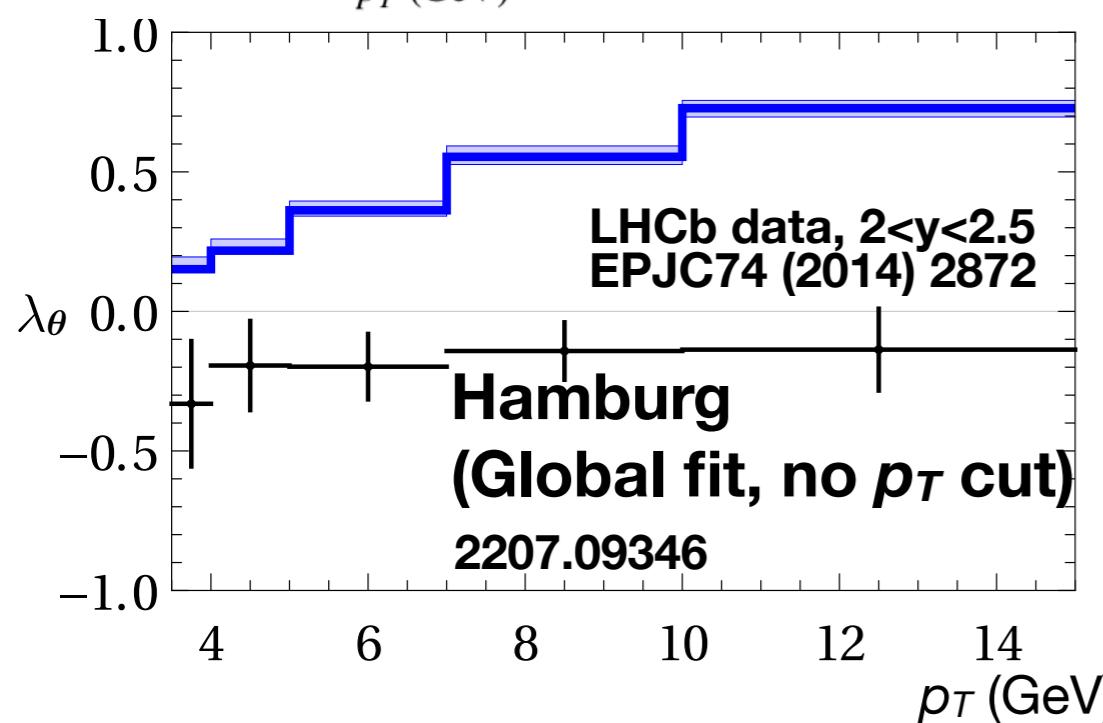
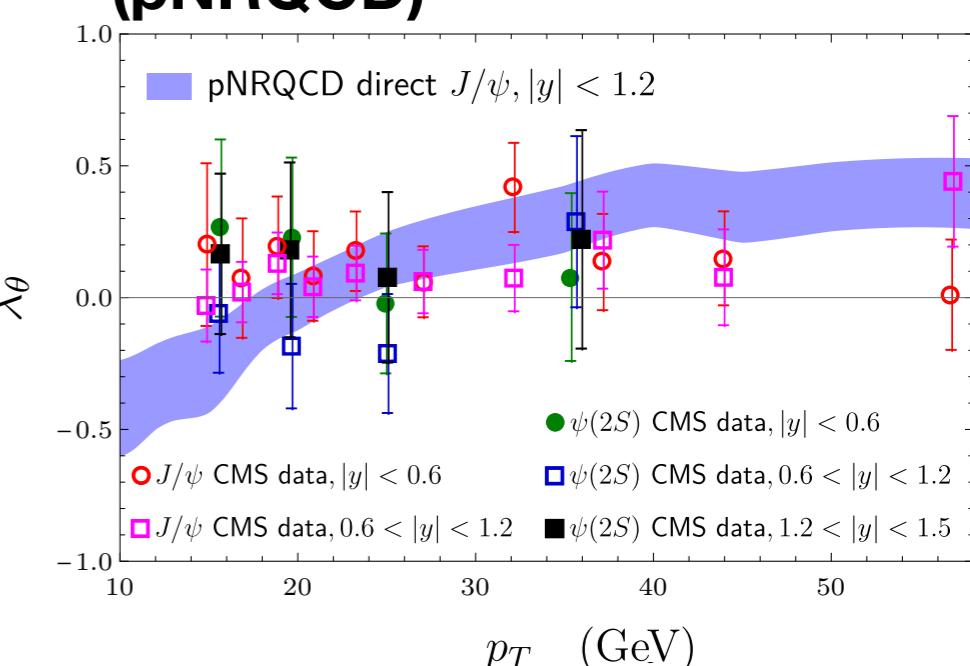
Peking PRD93, 034041 (2016)



TUM

(pNRQCD)

PRD105, L111503 (2022)

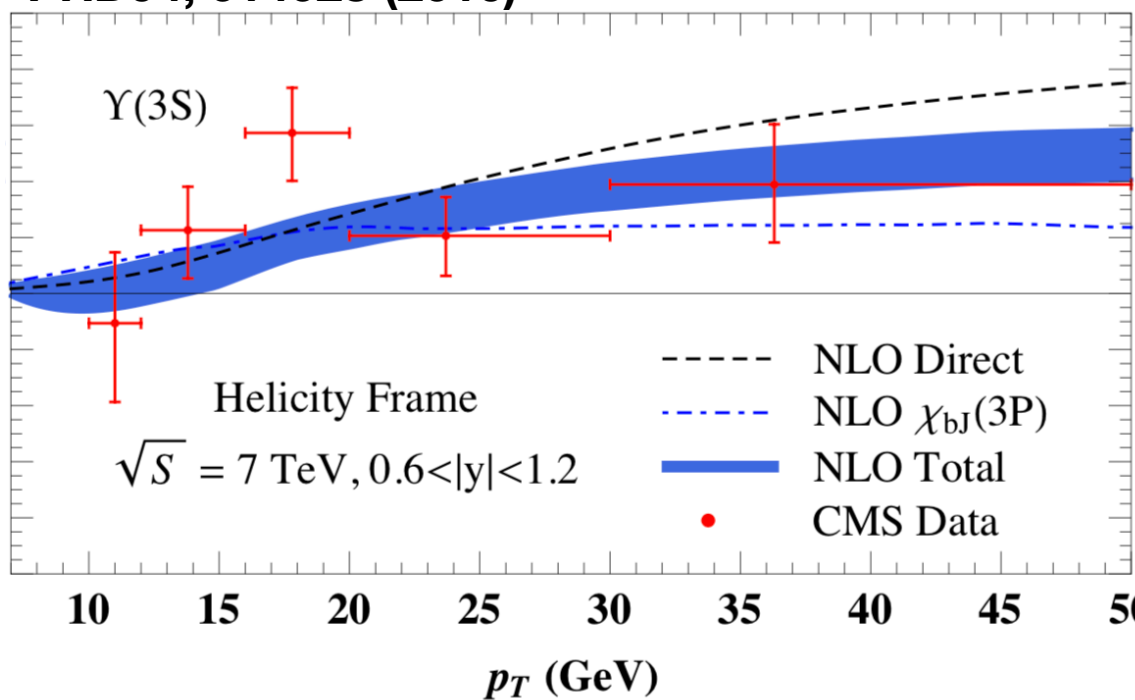


Υ Polarization

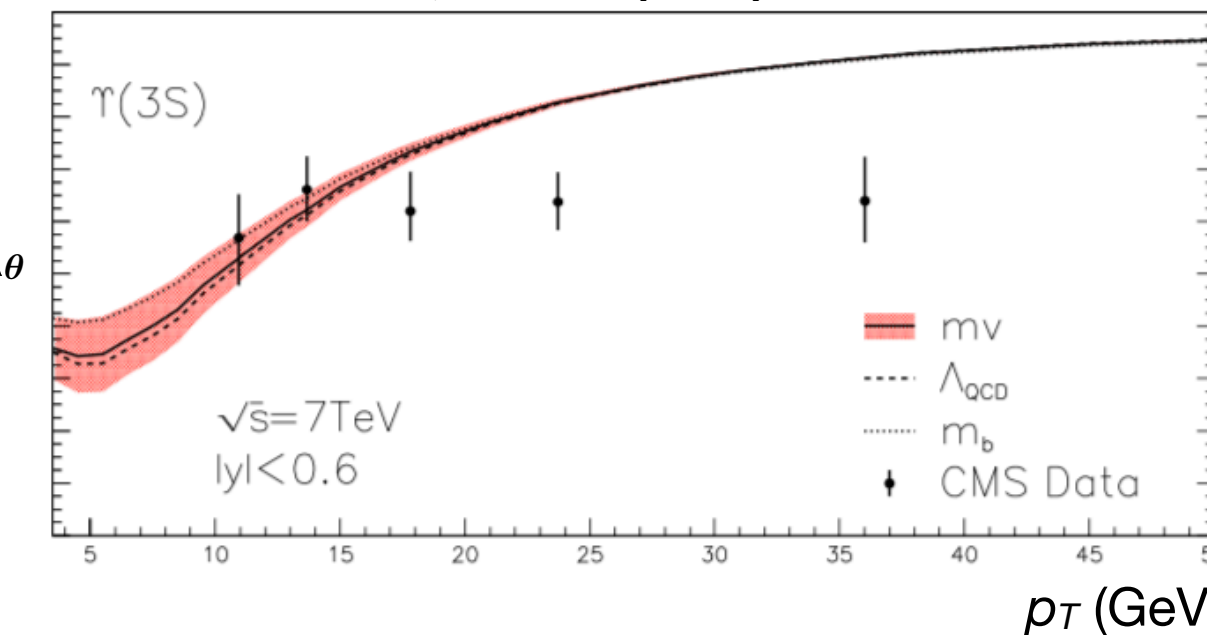
- Hadroproduction-based determinations generally lead to good descriptions of polarization.

Peking

PRD94, 014028 (2016)

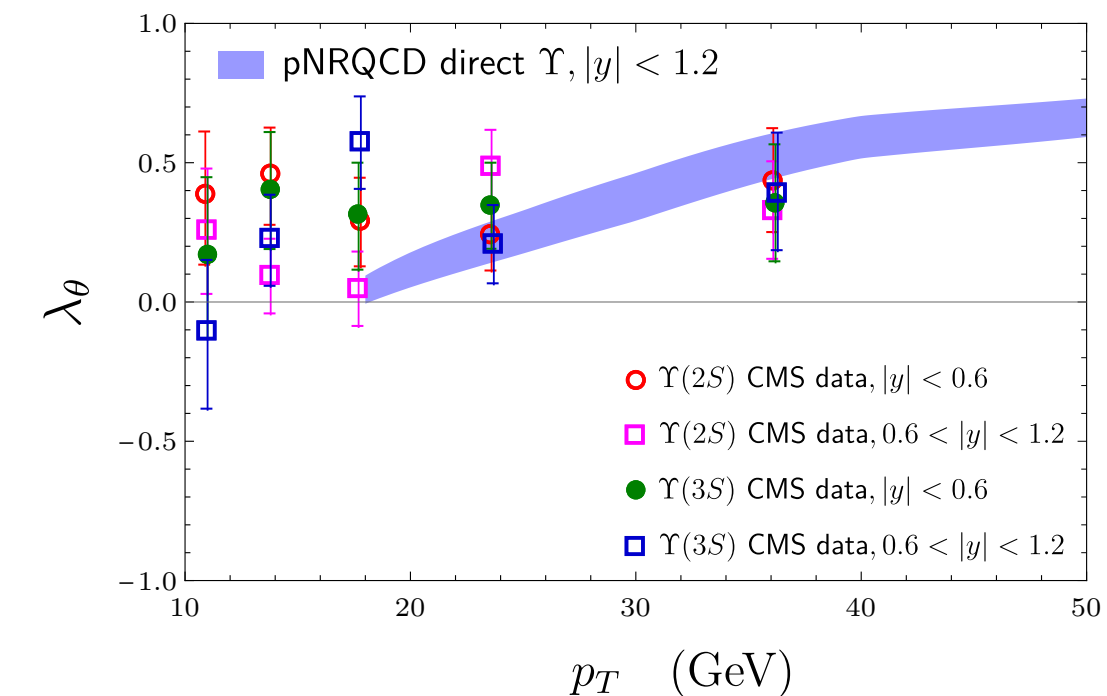


IHEP PRL112, 032001 (2014)



TUM

(pNRQCD) PRD105, L111503 (2022)



CMS PRL 110, 081802 (2013)

Other observables

- Polarization alone do not constrain color-octet matrix elements strongly, because near-zero λ_θ can be obtained from both $^3S_1[8]+^3P_J[8]$ dominance and $^1S_0[8]$ dominance scenarios.
- Hadroproduction-based analyses are usually between the two scenarios.
- pNRQCD analysis using universality of gluonic correlators leads to large positive $^3P_J[8]$, which favors $^3S_1[8]+^3P_J[8]$ dominance and small $^1S_0[8]$ for all 3S_1 quarkonia.
- Global fit analysis shows that low- p_T observables do not lead to polarization results consistent with measurements.
- Other large- p_T observables may be able to give additional constraints.

η_c Production

- By using heavy-quark spin symmetry, J/ψ matrix elements lead to η_c matrix elements

$$\begin{aligned}\sigma_{\eta_c+X} = & \hat{\sigma}_{Q\bar{Q}(^1S_0^{[1]})} \langle \mathcal{O}^{\eta_c}(^1S_0^{[1]}) \rangle + \hat{\sigma}_{Q\bar{Q}(^3S_1^{[8]})} \langle \mathcal{O}^{\eta_c}(^3S_1^{[8]}) \rangle \\ & + \hat{\sigma}_{Q\bar{Q}(^1S_0^{[8]})} \langle \mathcal{O}^{\eta_c}(^1S_0^{[8]}) \rangle + \hat{\sigma}_{Q\bar{Q}(^1P_1^{[8]})} \langle \mathcal{O}^{\eta_c}(^1P_1^{[8]}) \rangle\end{aligned}$$

- Significant contributions come from ${}^1S_0^{[1]}$ and ${}^3S_1^{[8]}$ channels.
(color singlet contribution is not suppressed)

Heavy-quark spin symmetry relations:

$$\langle \mathcal{O}^{\eta_c}(^1S_0^{[1]}) \rangle = \frac{1}{3} \times \langle \mathcal{O}^{J/\psi}(^3S_1^{[1]}) \rangle \quad \langle \mathcal{O}^{\eta_c}(^3S_1^{[8]}) \rangle = \langle \mathcal{O}^{J/\psi}(^1S_0^{[8]}) \rangle$$

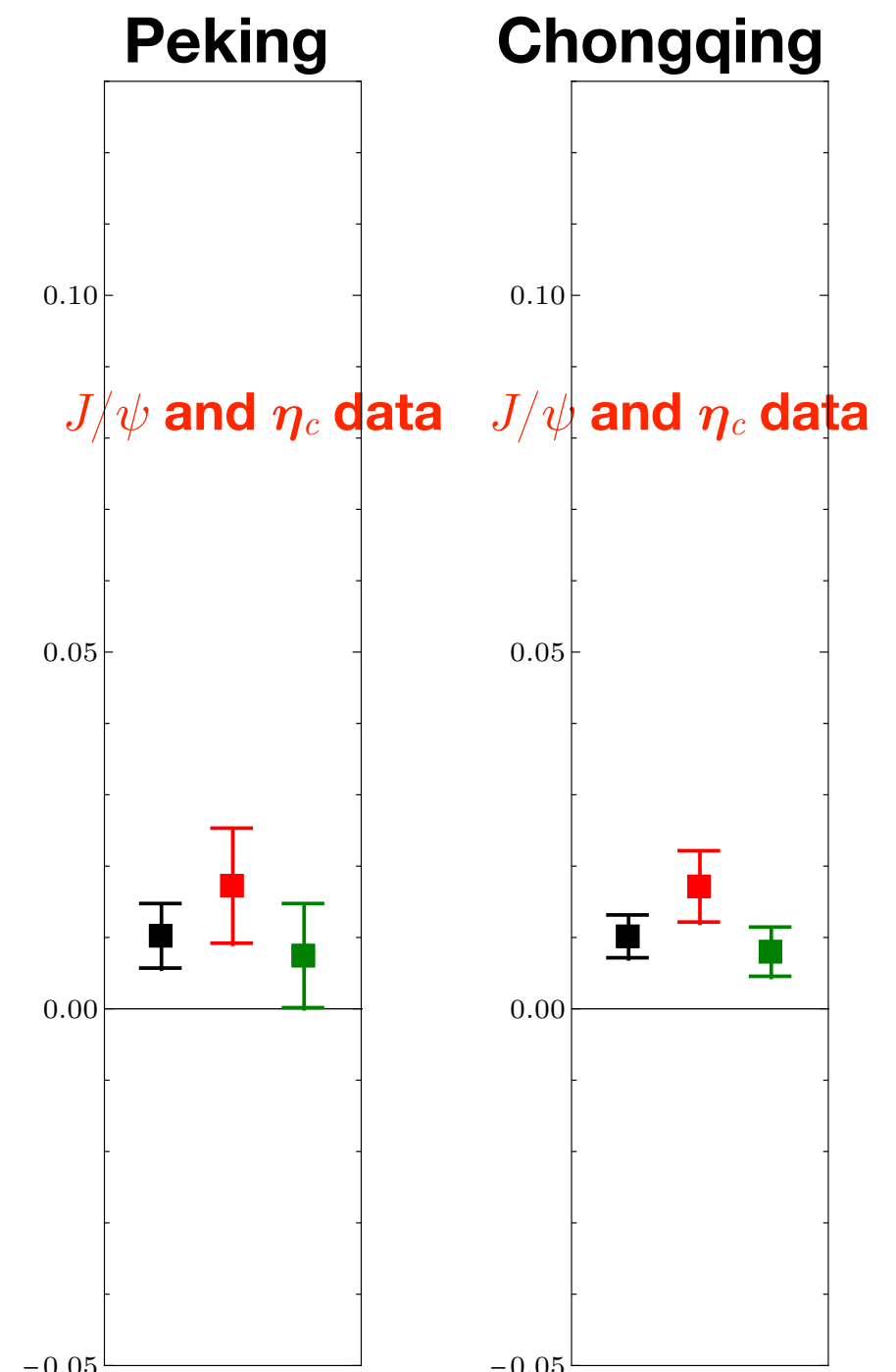
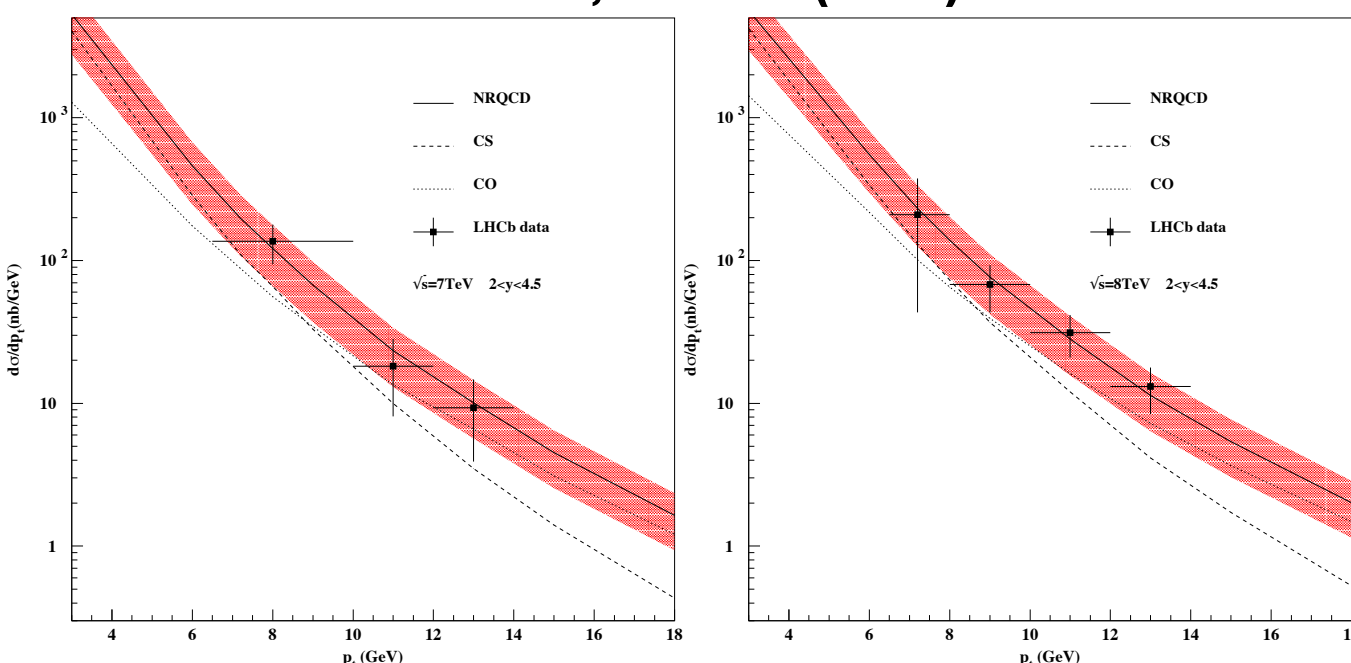
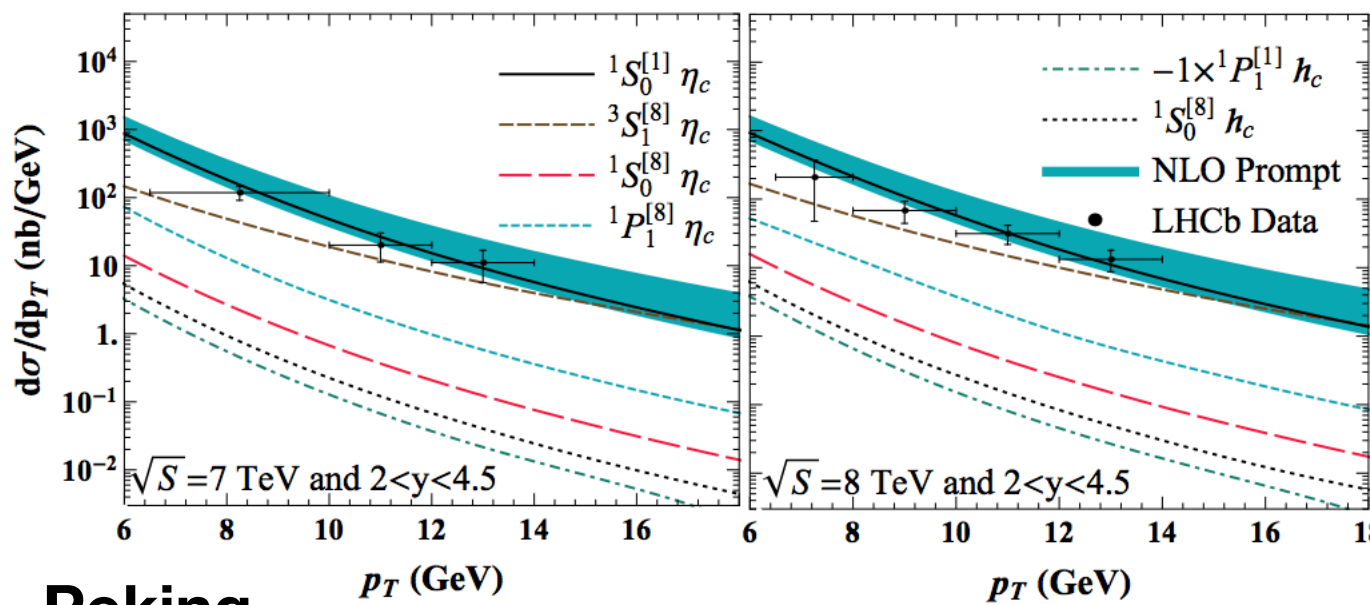
$$\langle \mathcal{O}^{\eta_c}(^1S_0^{[8]}) \rangle = \frac{1}{3} \times \langle \mathcal{O}^{J/\psi}(^3S_1^{[8]}) \rangle \quad \langle \mathcal{O}^{\eta_c}(^1P_1^{[8]}) \rangle = 3 \times \langle \mathcal{O}^{J/\psi}(^3P_0^{[8]}) \rangle$$

- This can be used to constrain $\langle \mathcal{O}^{\eta_c}(^3S_1^{[8]}) \rangle = \langle \mathcal{O}^{J/\psi}(^1S_0^{[8]}) \rangle$
- The production rate has been measured by LHCb

LHCb, EPJC75 (2015) 7, 311
EPJC80 (2020) 3, 191

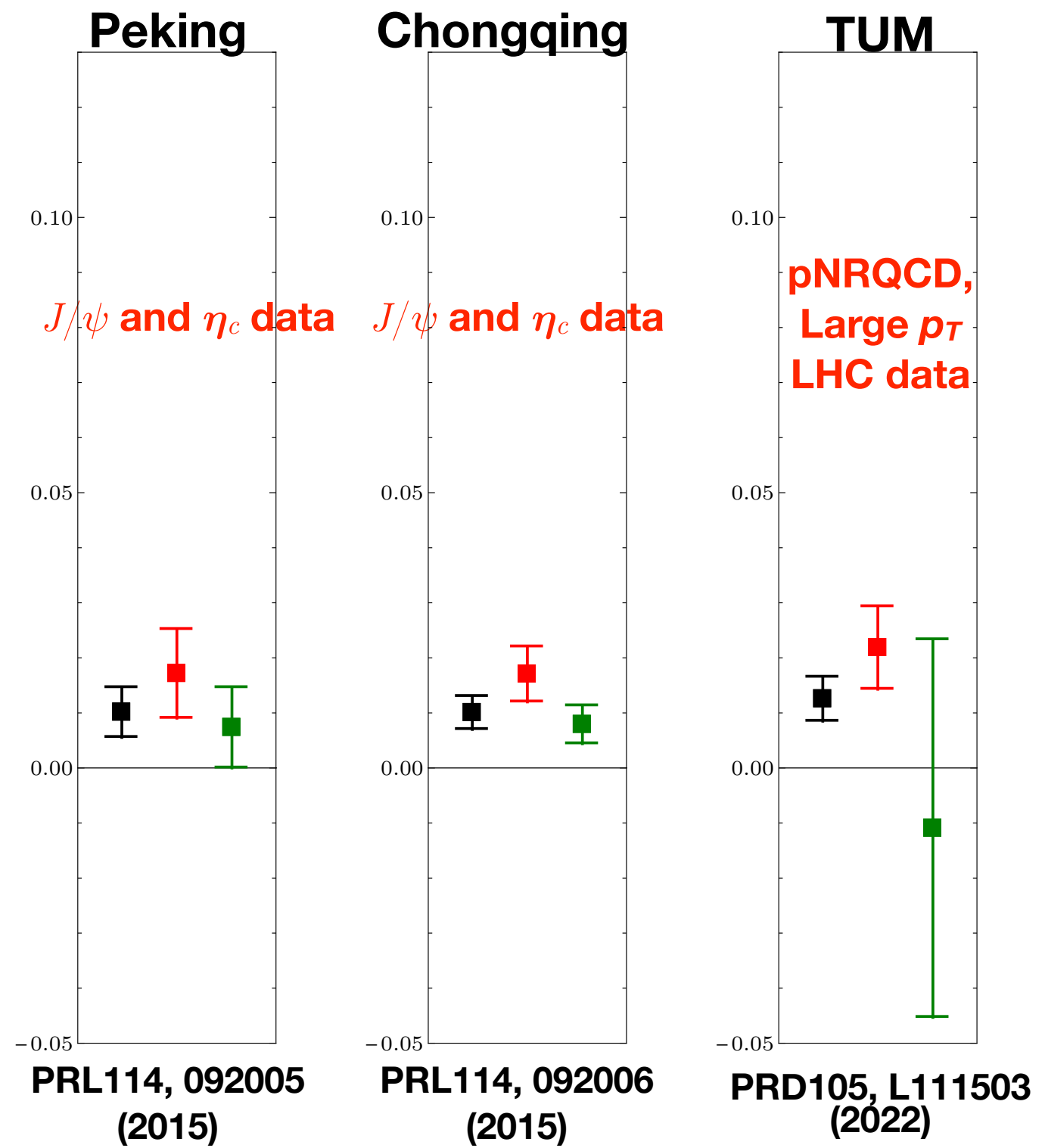
η_c Production

- Additional constraints from η_c production to J/ψ matrix elements $\langle \mathcal{O}^{J/\psi}(^3S_1^{[8]}) \rangle$ $\langle \mathcal{O}^{J/\psi}(^3P_0^{[8]}) \rangle/m^2$ $\langle \mathcal{O}^{J/\psi}(^1S_0^{[8]}) \rangle (\text{GeV}^3)$



J/ψ matrix elements

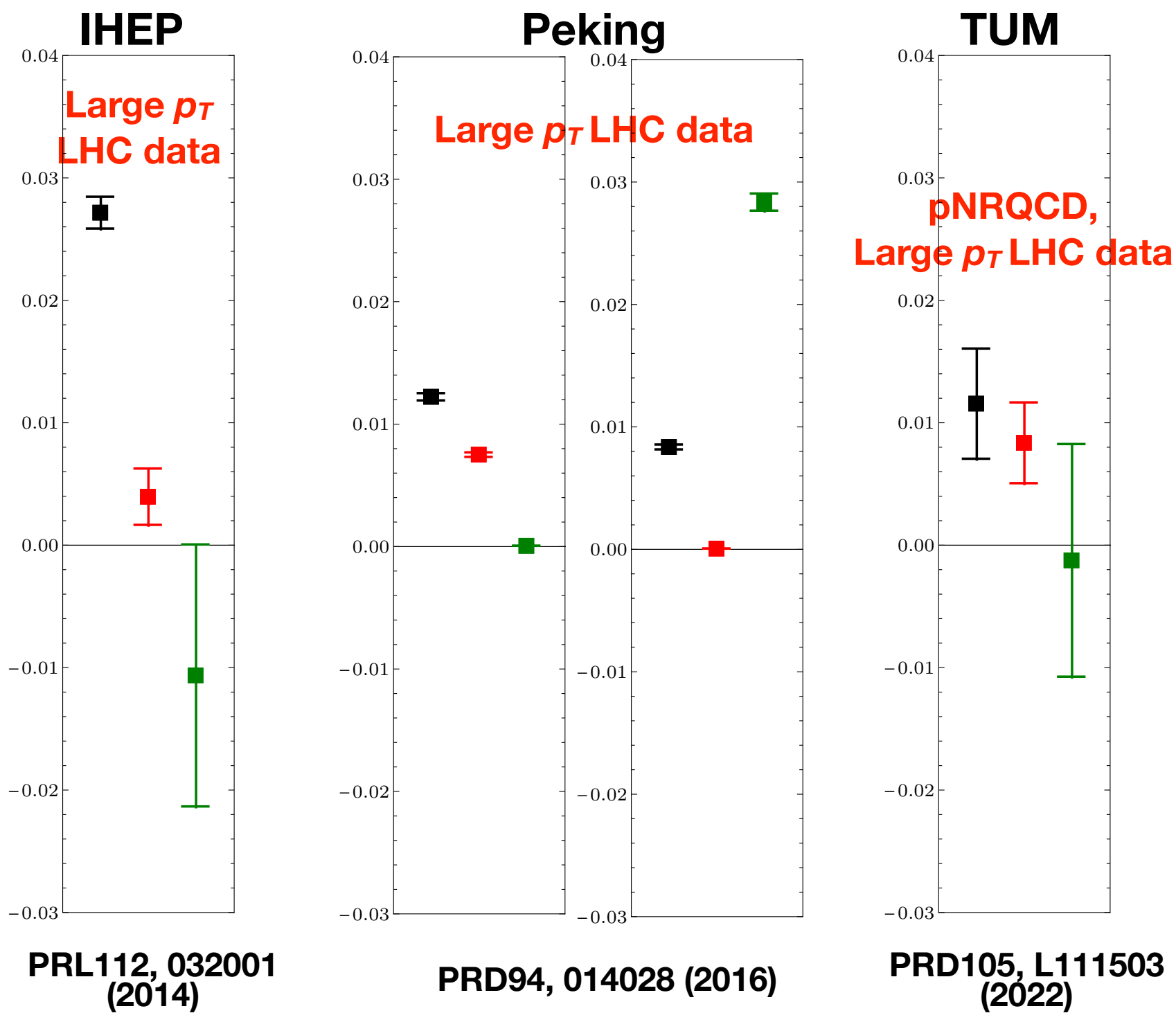
- J/ψ matrix elements $\langle \mathcal{O}^{J/\psi}(^3S_1^{[8]}) \rangle$ $\langle \mathcal{O}^{J/\psi}(^3P_0^{[8]}) \rangle/m^2$ $\langle \mathcal{O}^{J/\psi}(^1S_0^{[8]}) \rangle$
- Determinations with $^3S_1^{[8]} + ^3P_J^{[8]}$ dominance can describe cross sections, polarizations, η_c and associated production cross sections.
- pNRQCD implies similar results for all other 3S_1 quarkonium states.
- Caveat : inconsistent with low- p_T observables, large cancellations can be bad for perturbative stability



Υ matrix elements

- $\Upsilon(3S)$ matrix elements $\langle \mathcal{O}^\Upsilon(^3S_1^{[8]}) \rangle$ $\langle \mathcal{O}^\Upsilon(^3P_0^{[8]}) \rangle/m^2$ $\langle \mathcal{O}^\Upsilon(^1S_0^{[8]}) \rangle$ (GeV³)

- Υ matrix element determinations are still limited to cross section data.
- pNRQCD implies $^3S_1^{[8]} + ^3P_J^{[8]}$ dominance also for Υ states. Cancellation less severe than charmonium case due to running of $\langle \mathcal{O}^\Upsilon(^3S_1^{[8]}) \rangle$



Summary and outlook

- **NRQCD** description of J/ψ , $\psi(2S)$, Υ production depends heavily on determination of *three matrix elements* corresponding to $^3S_1[8]$, $^3P_J[8]$, $^1S_0[8]$.
- **pNRQCD** gives *universality relations* that reduce the number of independent matrix elements through universality of gluonic correlators.
- Polarization is still useful for testing matrix elements, but cannot strongly distinguish $^3S_1[8]+^3P_J[8]$ dominance and $^1S_0[8]$ dominance.
- This degeneracy can be lifted from
 - **pNRQCD theory** supports $^3S_1[8]+^3P_J[8]$ dominance for all 3S_1 quarkonia
 - J/ψ and η_c data also support $^3S_1[8]+^3P_J[8]$ dominance for J/ψ .
- On the other hand, large p_T determinations are in conflict with low- p_T observables. $^3S_1[8]+^3P_J[8]$ dominance also prone to radiative corrections.
- $J/\psi+W/Z$ measurements and future experiments such as the EIC can provide useful tests of the quarkonium production mechanism.

Backup

Potential NRQCD

- Definitions of gluonic correlators:

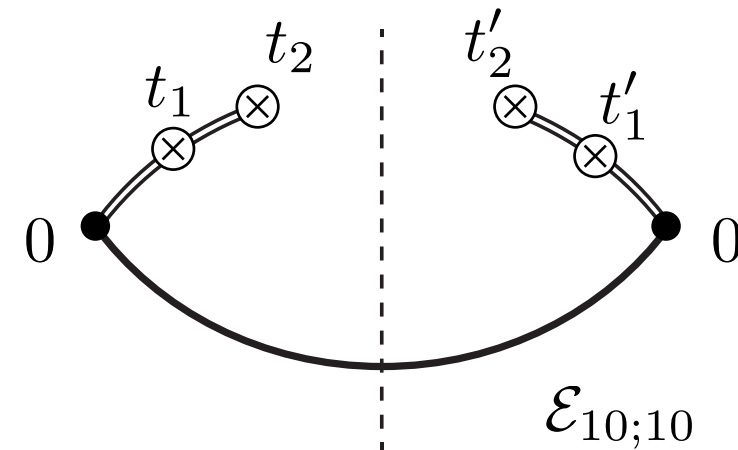
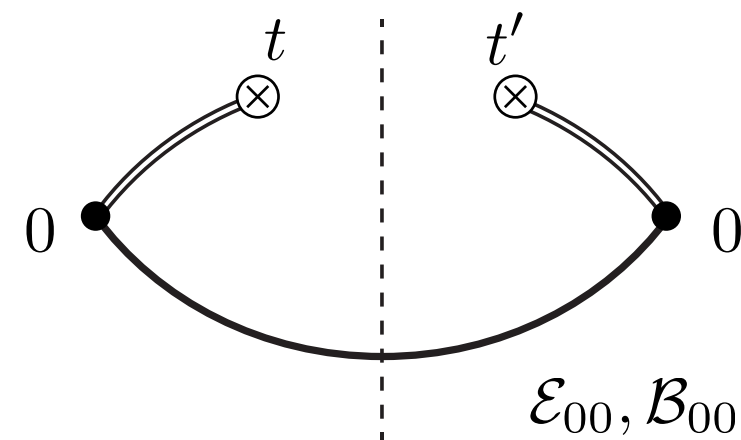
$$\mathcal{E}_{10;10} = d^{a'b c'} d^{e' x y'} \int_0^\infty dt_1 t_1 \int_{t_1}^\infty dt_2 \langle \Omega | \Phi_\ell^{\dagger ad}(0) \Phi_0^{a' a\dagger}(0; t_1) g E^{b,i}(t_1) \Phi_0^{c c'\dagger}(t_1; t_2) g E^{c,i}(t_2)$$

$$\times \int_0^\infty dt'_1 t'_1 \int_{t'_1}^\infty dt'_2 g E^{y,j}(t'_2) \Phi_0^{y y'}(t'_1; t'_2) g E^{x,j}(t'_1) \Phi_0^{e' e}(0; t'_1) \Phi_\ell^{d e}(0) | \Omega \rangle$$

$$\mathcal{E}_{00} = \int_0^\infty dt \int_0^\infty dt' \langle \Omega | \Phi_\ell^{\dagger ab}(0) \Phi_0^{\dagger ad}(0; t) g E^{d,i}(t) g E^{e,i}(t') \Phi_0^{e c}(0; t') \Phi_\ell^{b c}(0) | \Omega \rangle$$

$$\mathcal{B}_{00} = \int_0^\infty dt \int_0^\infty dt' \langle \Omega | \Phi_\ell^{\dagger ab}(0) \Phi_0^{\dagger ad}(0; t) g B^{d,i}(t) g B^{e,i}(t') \Phi_0^{e c}(0; t') \Phi_\ell^{b c}(0) | \Omega \rangle$$

- Configurations of Wilson lines and field strength insertions:



Υ Polarization and evolution

- Υ is generally more transverse than ψ at similar values of p_T/m . This happens because the relative size of ${}^3S_1[8]$ compared to ${}^3P_J[8]$ is larger for bottomonium than charmonium.
- The evolution equation :

$$\langle \mathcal{O}^V({}^3S_1[8]) \rangle^{(\Lambda)} = \frac{1}{2N_c m^2} \frac{3|R(0)|^2}{4\pi} \mathcal{E}_{10;10}(\Lambda) \quad \langle \mathcal{O}^V({}^3P_0[8]) \rangle = \frac{1}{18N_c} \frac{3|R(0)|^2}{4\pi} \mathcal{E}_{00}$$

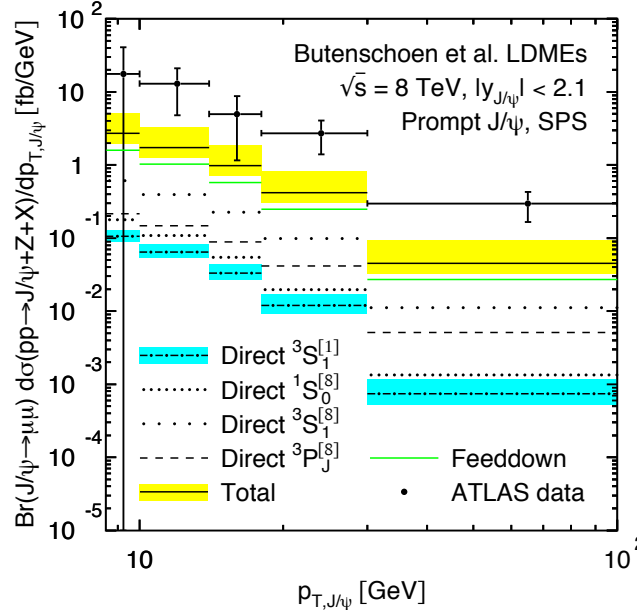
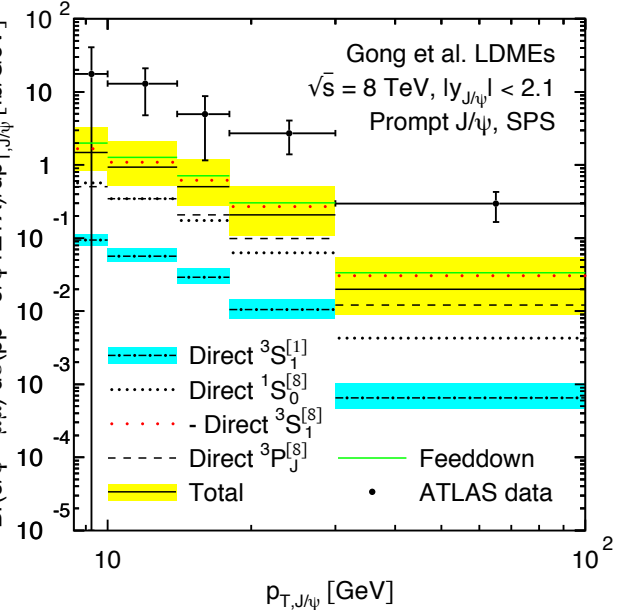
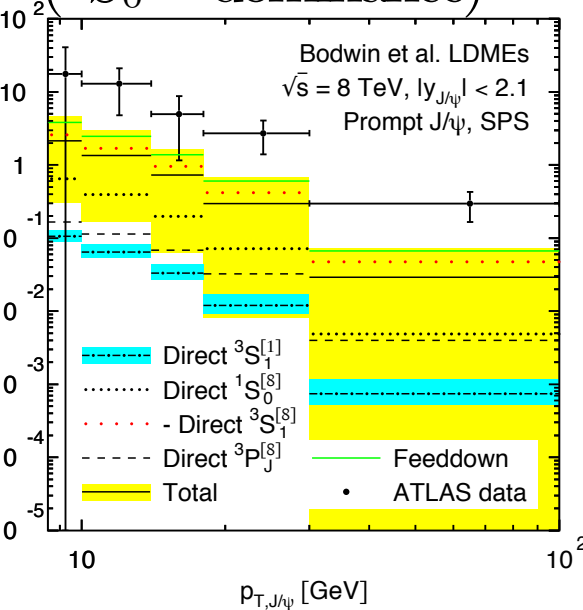
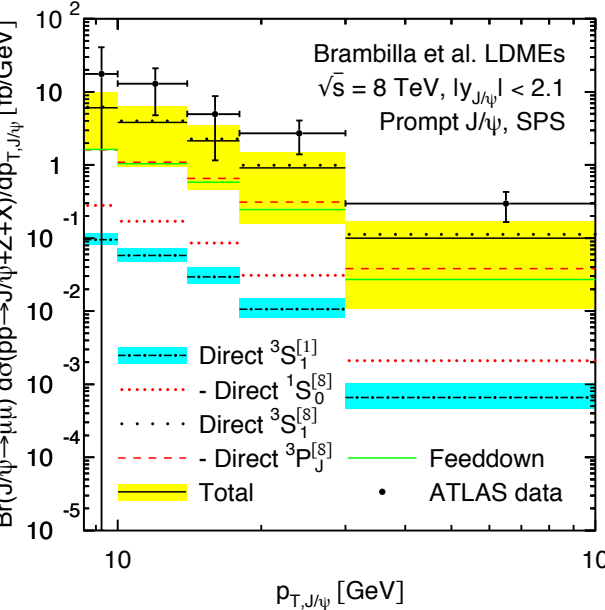
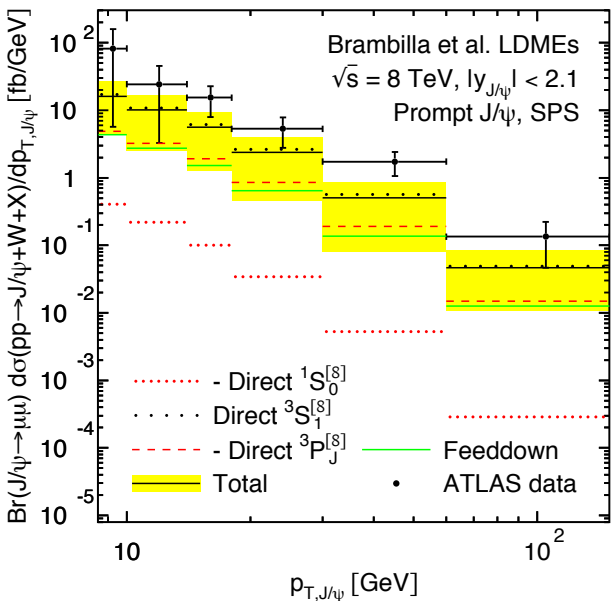
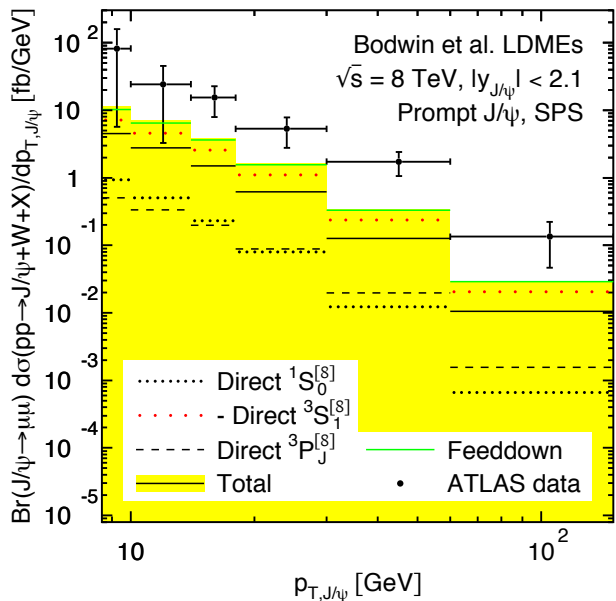
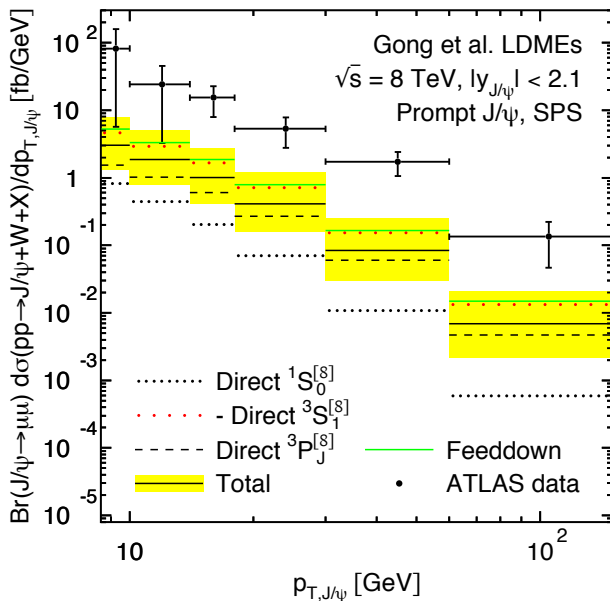
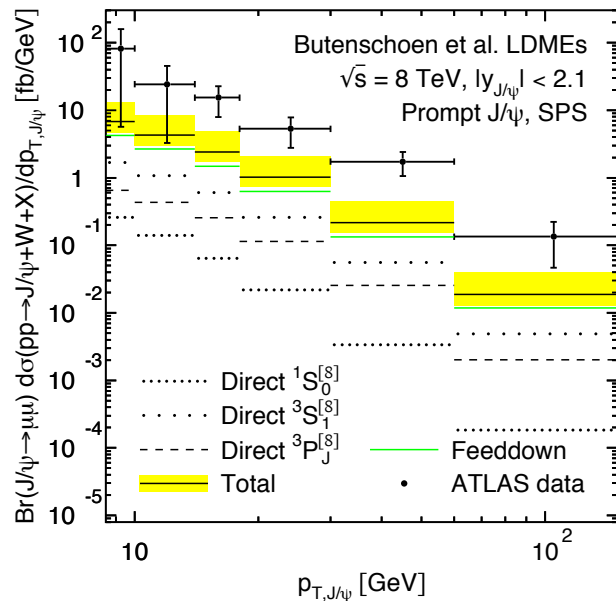
$$\frac{d}{d \log \Lambda} \mathcal{E}_{10;10} = \frac{2\alpha_s}{3\pi} \frac{N_c^2 - 4}{N_c} \mathcal{E}_{00}$$

For ${}^3S_1[8]$ to be larger at $\Lambda=m_b$ than at $\Lambda=m_c$, ${}^3P_J[8]$ needs to be positive.

- Hence pNRQCD strongly constrains ${}^3P_J[8]$ to be positive. To counter the large negative ${}^3P_J[8]$ contribution, large positive contribution should come from the ${}^3S_1[8]$ channel, leading to ${}^3S_1[8]+{}^3P_J[8]$ dominance.

$J/\psi + W/Z$ Production

- Associated production can also help discriminate matrix elements : ATLAS measured $J/\psi + W$ and $J/\psi + Z$ production
ATLAS, EPJC75 (2015) 229, JHEP 01 (2020) 095, JHEP 04 (2014) 172

Hamburg (Global fit)**IHEP (${}^1S_0[8]$ dominance)****ANL/KU/Peking (${}^1S_0[8]$ dominance)****TUM (pNRQCD)** **$J/\psi + Z$** 

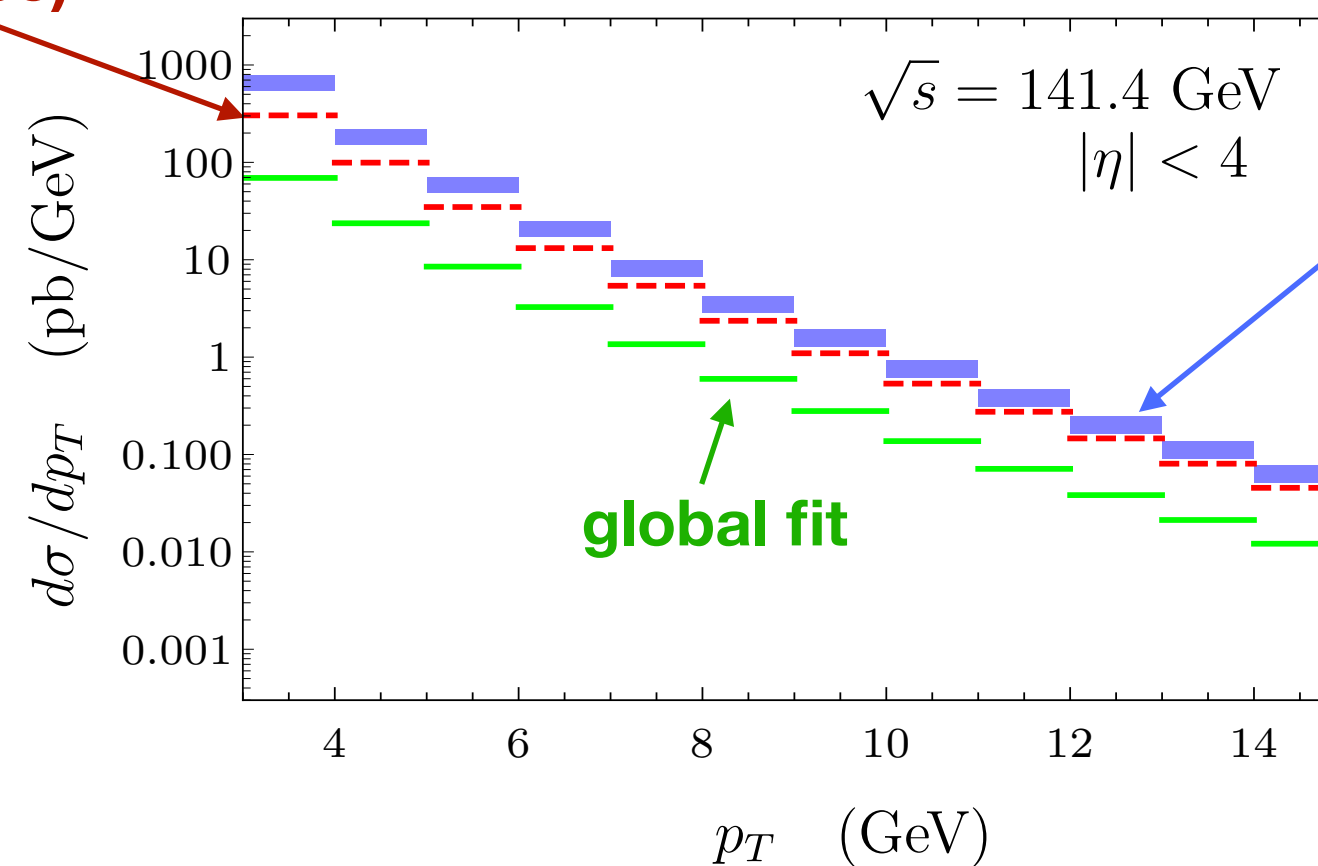
Butenschoen and Kniehl, 2207.09366

J/ψ Production at EIC

- The $ep \rightarrow J/\psi + X$ cross section can also discriminate different matrix element determinations, and is expected to be measurable at the EIC.

IHEP

($^1S_0[8]$ dominance)

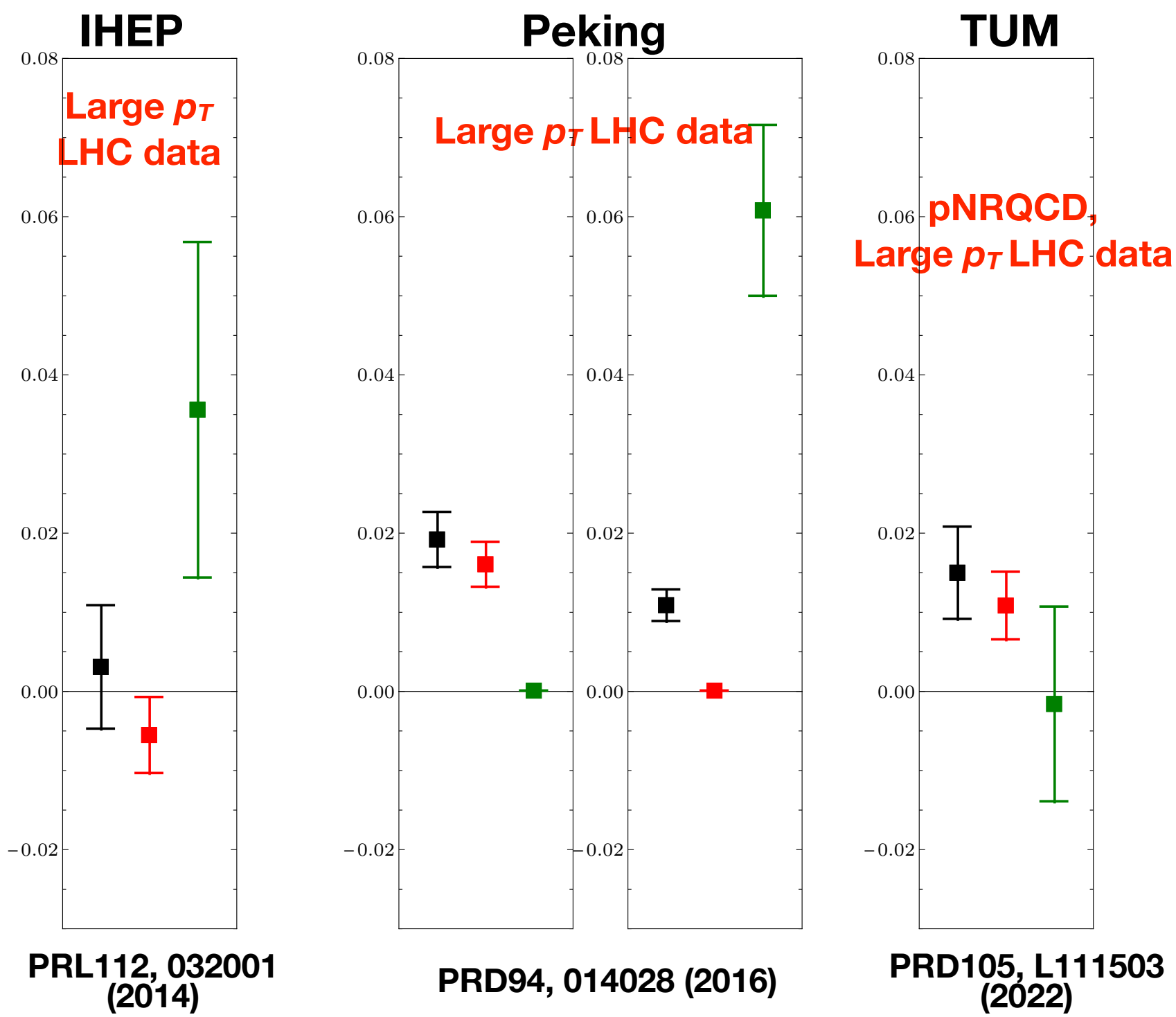


pNRQCD (preliminary)
($^3S_1[8] + ^3P_J[8]$ dominance)

Short-distance coefficients from
Qiu, Wang, Xing, Chin. Phys. Lett. 38 (2021) 041201

Υ matrix elements

- $\Upsilon(2S)$ matrix elements $\langle \mathcal{O}^\Upsilon(^3S_1^{[8]}) \rangle$ $\langle \mathcal{O}^\Upsilon(^3P_0^{[8]}) \rangle/m^2$ $\langle \mathcal{O}^\Upsilon(^1S_0^{[8]}) \rangle$ (GeV³)
- IHEP determination has poor description of P-wave feeddowns
- pNRQCD implies $^3S_1^{[8]} + ^3P_J^{[8]}$ dominance also for Υ states.
Cancellation less severe than charmonium case due to running of $\langle \mathcal{O}^\Upsilon(^3S_1^{[8]}) \rangle$



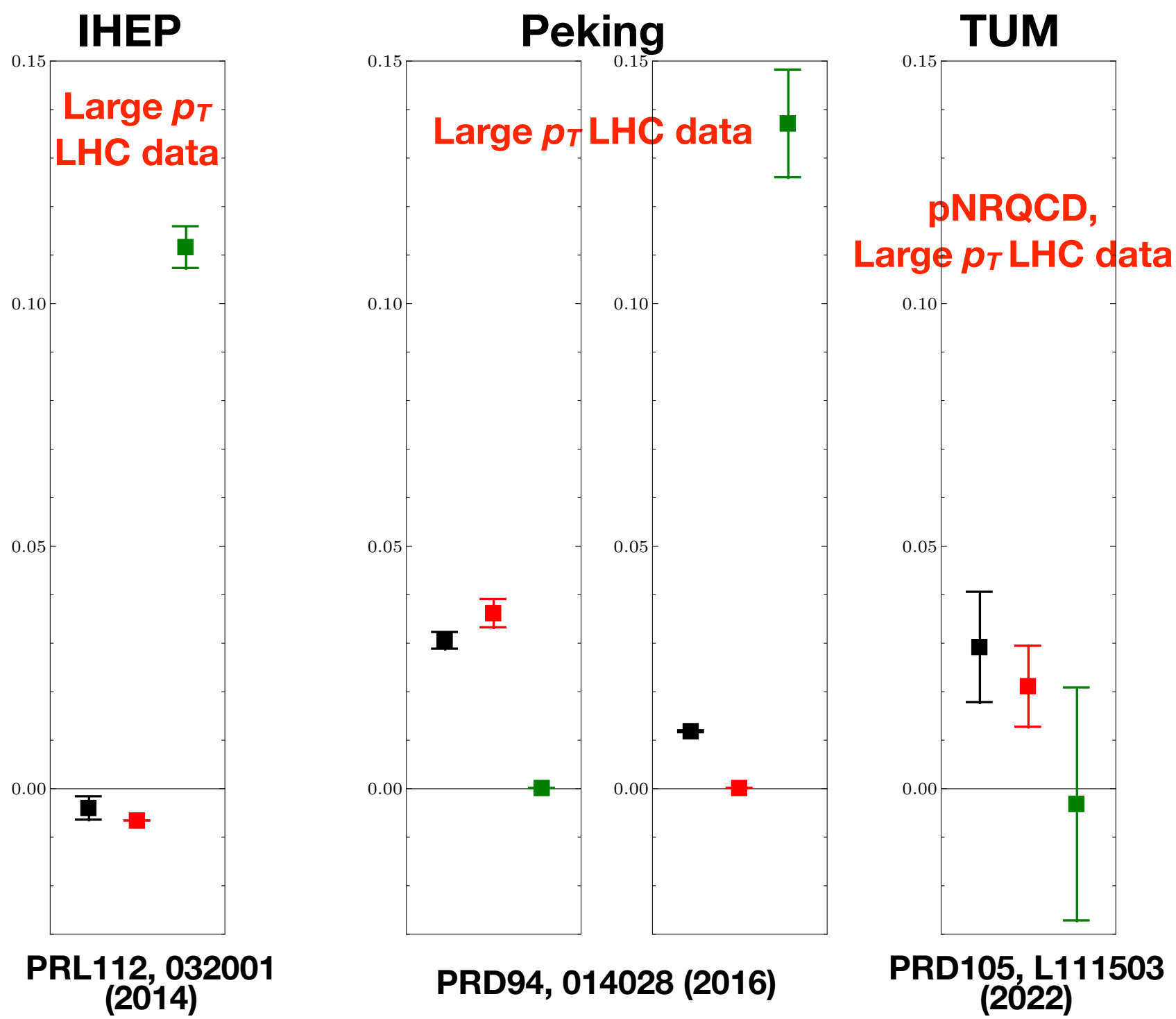
Υ matrix elements

- $\Upsilon(1S)$ matrix elements $\langle \mathcal{O}^\Upsilon(^3S_1^{[8]}) \rangle$ $\langle \mathcal{O}^\Upsilon(^3P_0^{[8]}) \rangle/m^2$ $\langle \mathcal{O}^\Upsilon(^1S_0^{[8]}) \rangle$ (GeV³)

- IHEP determination has poor description of P-wave feeddowns

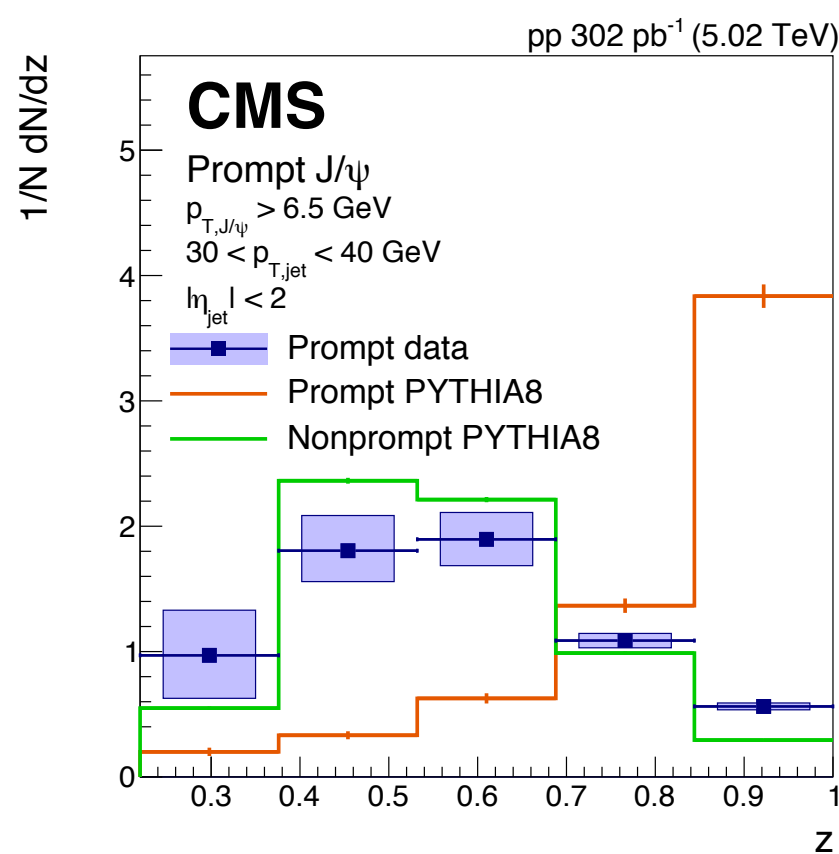
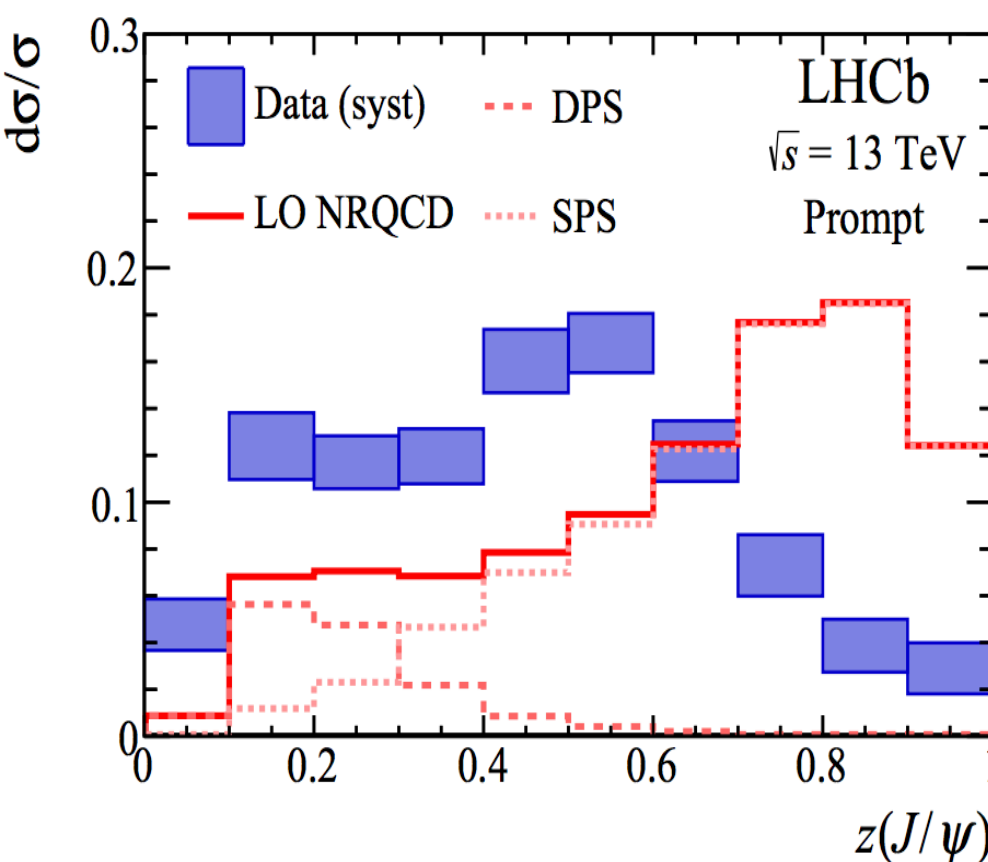
- pNRQCD implies $^3S_1^{[8]} + ^3P_J^{[8]}$ dominance.

Caveat : strongly coupled formalism may not be applicable for $\Upsilon(1S)$.



J/ψ in Jet

- J/ψ momentum distribution in jet have been measured by LHCb and CMS.
- LHCb, PRL118, 192001 (2017)
CMS, PLB 825 (2021) 136842

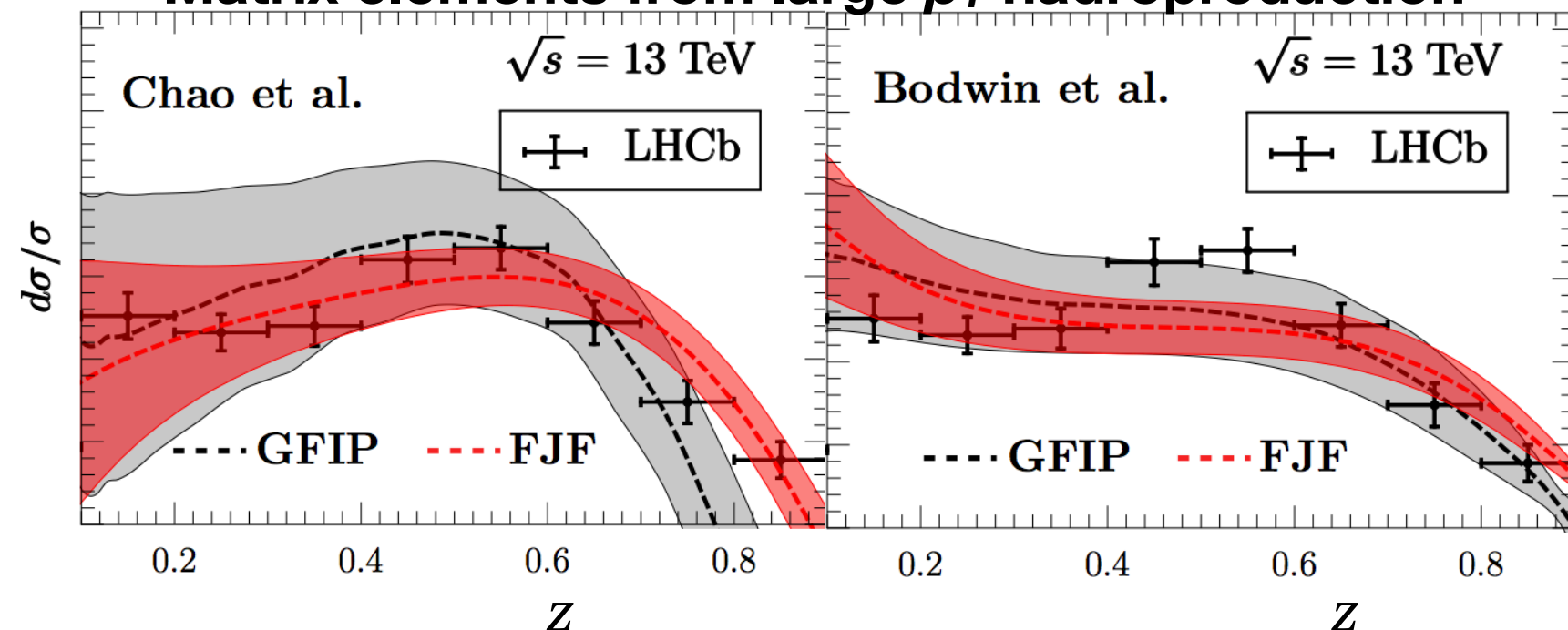


- $z = \text{fraction of } J/\psi \text{ transverse momentum in jet}$
- Measured distributions fall as $z \rightarrow 1$.

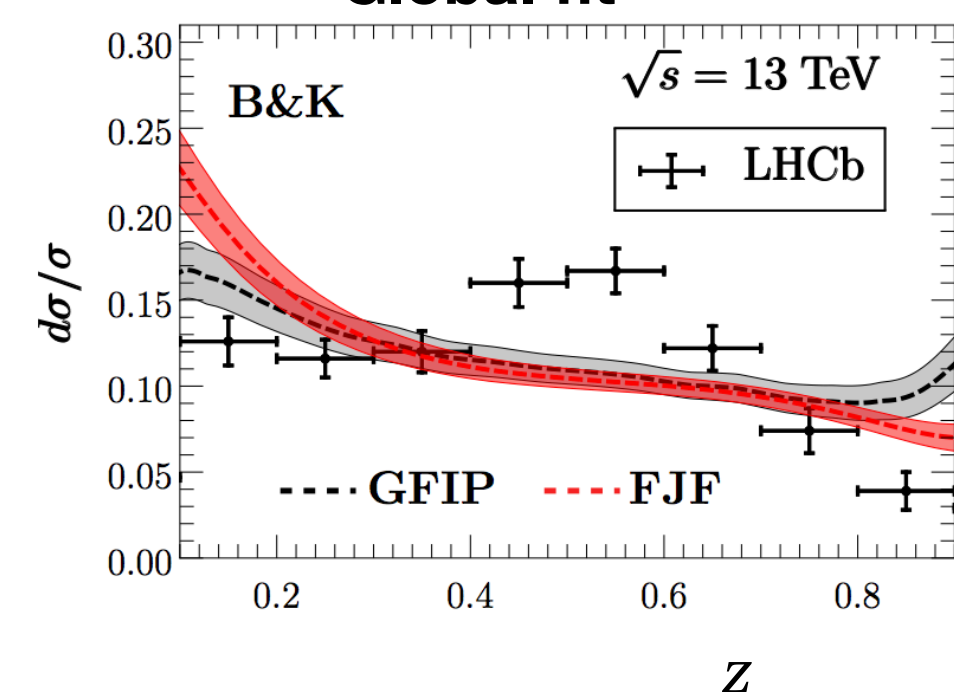
J/ψ in Jet

- The distribution has been studied in SCET (Fragmenting Jet Functions, FJF) and in gluon fragmentation improved PYTHIA (GFIP). Bain, Dai, Leibovich, Makris, Mehen, PRL119, 032002 (2017)

Matrix elements from large p_T hadroproduction



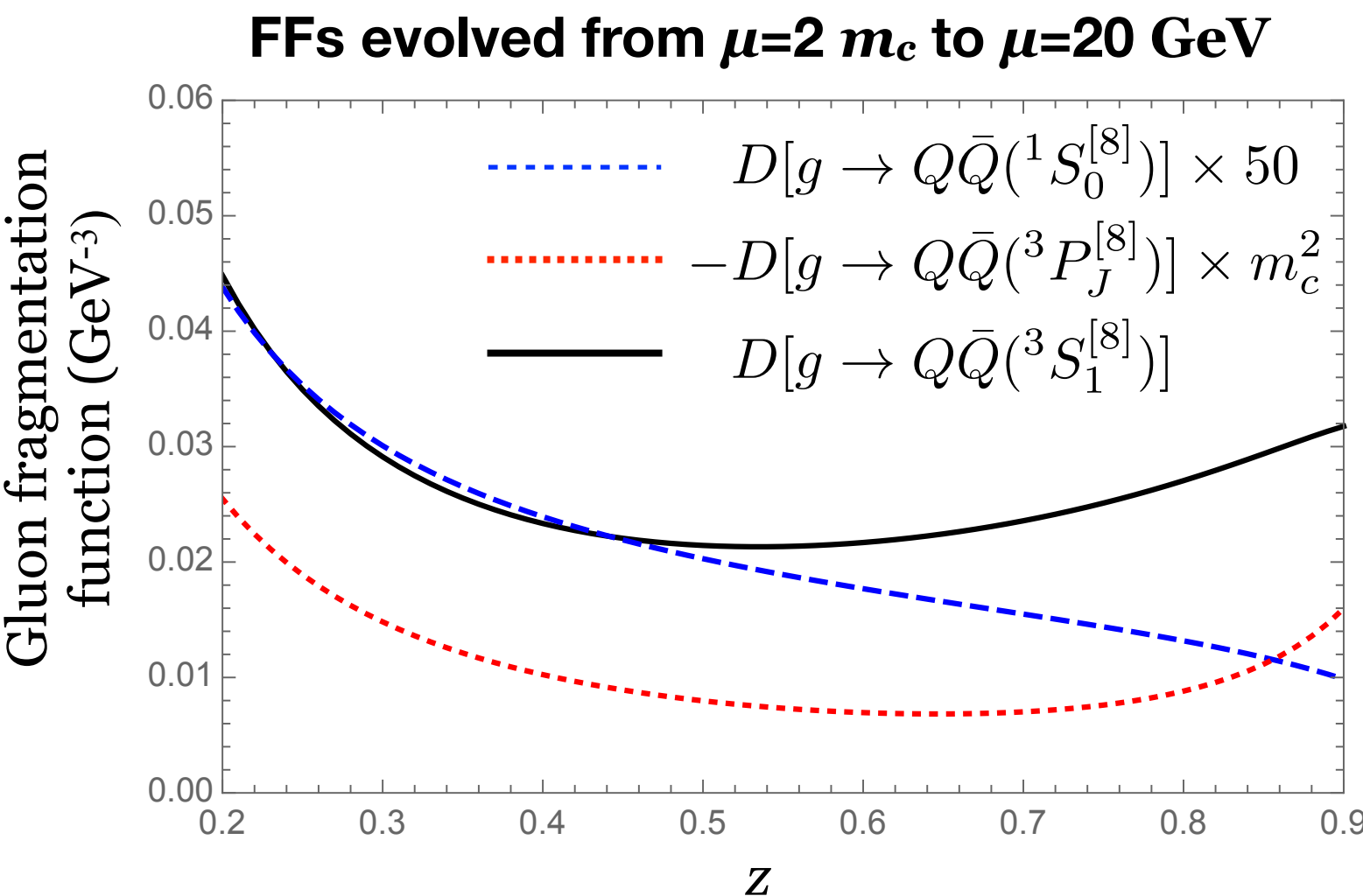
Global fit



- Data agrees better with theory when $^3S_1[8]$ and $^3P_J[8]$ matrix elements have same signs.

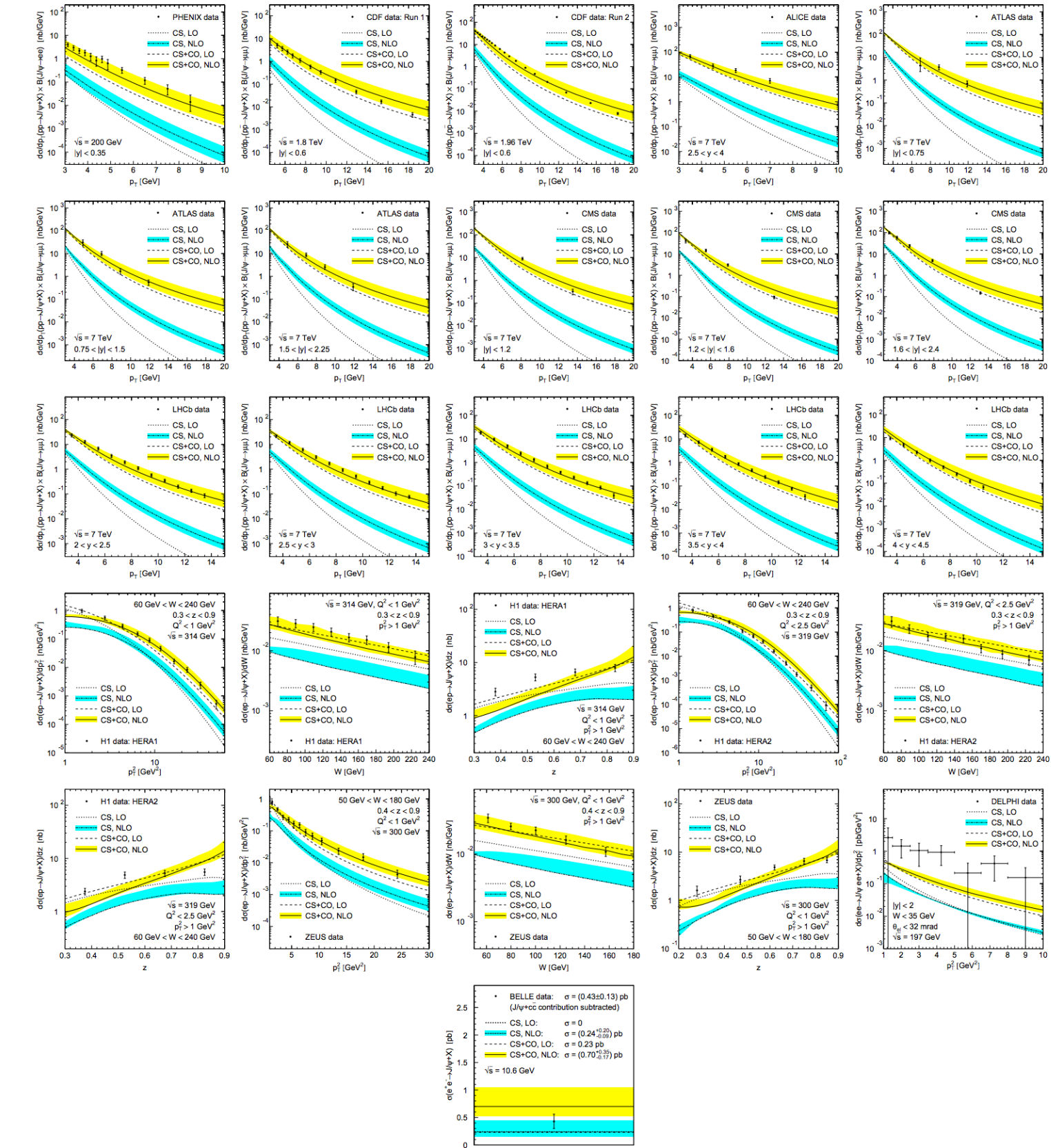
J/ψ in Jet

- At LO in α_s , the distribution is determined by the gluon fragmentation function. Fragmentation functions for $^3S_1^{[8]}$ and $^3P_J^{[8]}$ channels diverge as $z \rightarrow 1$.



- Hence, contributions from $^3S_1^{[8]}$ and $^3P_J^{[8]}$ channels must cancel to have decreasing distribution as $z \rightarrow 1$.

Global Fit



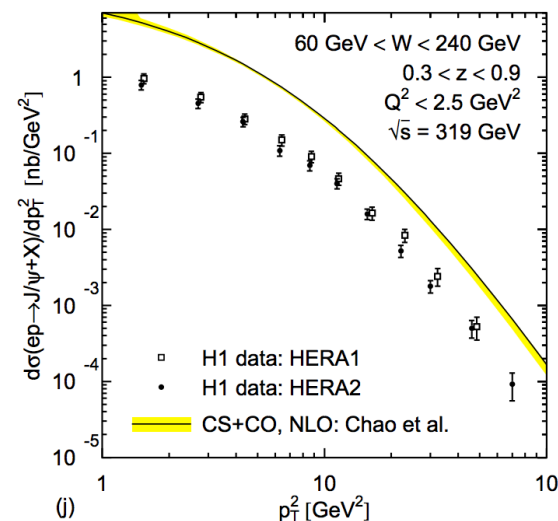
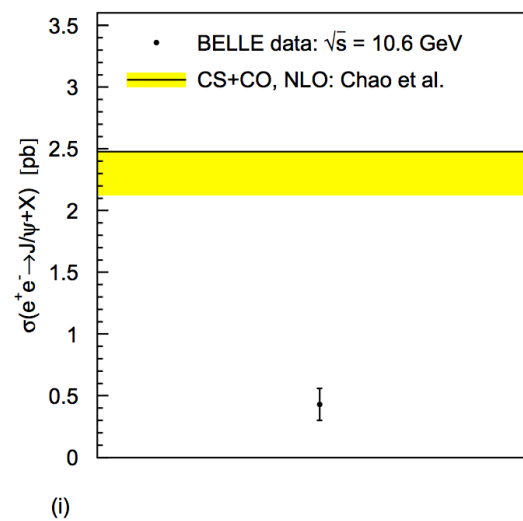
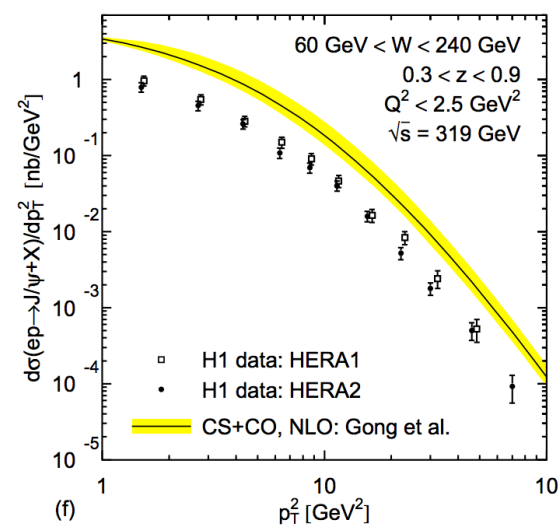
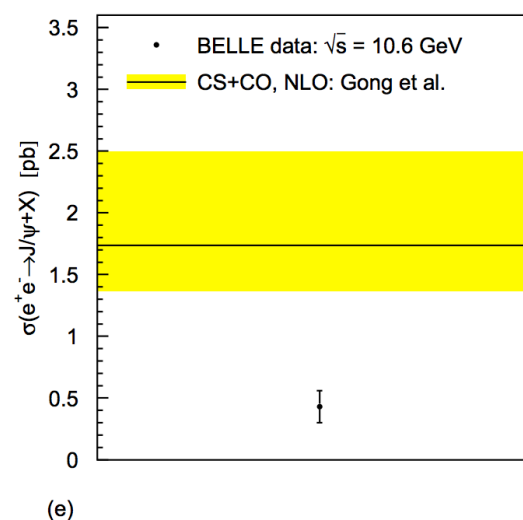
- Hadroproduction data from PHENIX at RHIC, CDF at Tevatron, ATLAS, CMS, ALICE and LHCb at LHC, (mostly at low p_T)
- Photoproduction data from ZEUS and H1 at HERA,
- DELPHI at LEP II, and Belle at KEKB.

Butenschoen and Kniehl,
MPLA28, 1350027 (2013)

Low- p_T observables

- Color-octet matrix elements extracted from hadroproduction data at large p_T lead to overestimation of photoproduction and Electromagnetic production data.

**Butenschoen and Kniehl,
MPLA28, 1350027 (2013)**



**Matrix elements from
Gong, Wan, Wang, Zhang,
PRL110, 042002 (2013)
(IHEP)**

**Matrix elements from
Chao, Ma, Shao, Wang, Zhang,
PRL108, 242004 (2012)
(Peking)**